Chapter 4. DC Glow Discharges

So far we have been dealing with a rather idealized homogeneous plasma with a well-defined potential and density, and with constituent particles in equilibrium motion characterized by relevant temperatures. The glow discharges which we're using only approximate this condition, for various reasons which we shall be discussing. Nevertheless, many of the plasma concepts are of great utility in helping us to derive some understanding and control of glow discharge processes, even on a semi-quantitative basis. Amongst sputtering and plasma etching folks, the words 'plasma' and 'glow discharge' tend to be used synonymously – to the horror of plasma physicists, I'm sure! One can get into semantic discussions and argue that some discharges are plasmas with two or three different groups of electrons each with a well-defined temperature. That argument could probably be extended indefinitely. So let's accept that our glow discharges are certainly not ideal plasmas, and keep this in mind when we lapse into glow discharge – plasma synonyms.

One of the complicating factors in trying to understand glow discharges is that most of the literature, particularly the 'classical' literature of the 1920's and 30's, deals with dc discharges; whereas practical plasma processes are more usually rf excited. And, as we said above, none of our practical glow discharges are truly plasmas. This gives then, in a sense, a choice: we can either pursue some plasma physics rather exactly, and then find that it does not entirely apply to our systems; or we can follow some simpler, if not always entirely accurate, models which convey the physical ideas rather well and, in the event, are probably just as accurate. In the present book I have opted for the latter.

Before commencing battle, I would recommend reading a delightful history of gaseous electronics by Brown (1974). Prof. Brown tells, for example, the story of the unfortunate pioneer Hittorf who laboured week after week, gradually extending the length of a thin glass discharge tube to try to discover the length of the positive column. Eventually the tube ran back and forth across Hittorf's laboratory. At this stage, a frightened cat pursued by a pack of dogs came flying through the window . . . "Until an unfortunate accident terminated my experiment", Hittorf wrote, "the positive column appeared to extend without limit."

ARCHITECTURE OF THE DISCHARGE

We could make a dc glow discharge by applying a potential between two electrodes in a gas; Figure 4-1 shows the resulting current density j flowing due to the application of a dc voltage V between a chromium cathode and a stainless steel anode, in argon gas at two different pressures. Each electrode was 12.5 cm diameter, and the electrodes were 6.4 cm apart. Most of the space between the two electrodes is filled by a bright glow known as the *negative glow*, the result of the excitation and subsequent recombination processes we discussed in Chapter 2. Adjacent to the cathode is a comparatively dark region known as the *dark space*. This corresponds to the sheath formed in front of the cathode; there is a similar sheath at the anode, but it is too thin to clearly see.

In this chapter, we shall be looking at dc discharges. These are somewhat easier to begin to analyze than rf discharges, although they are still extremely complex and we certainly don't understand all the details. Fortunately, much of what we learn can also be applied to rf systems.

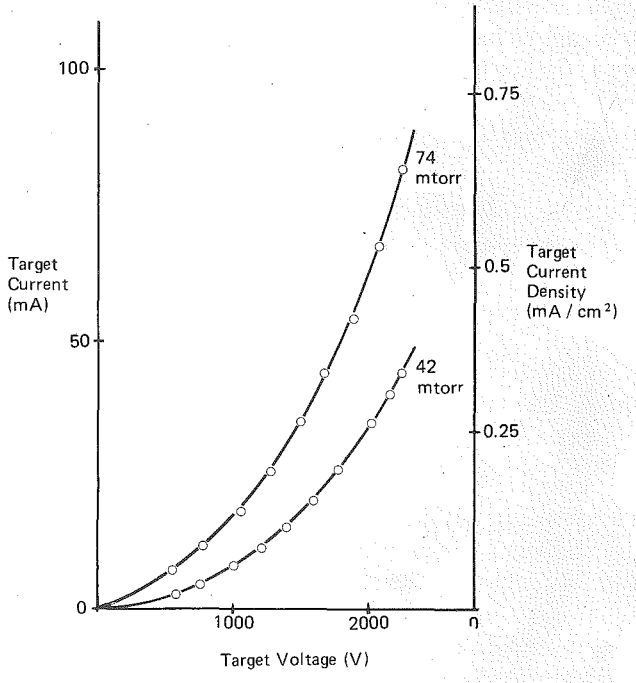

Figure 4-1. I-V characteristics for chromium sputtering in argon (Chapman 1975)

Many textbooks show a whole series of glowing and dark spaces in dc discharges. Figure 4-2 is from Nasser (1971); virtually the same figure appears in Cobine (1958), von Engel (1965) and doubtless many other texts. The *positive column* is the region of the discharge which most nearly resembles a plasma, and most of the classic probe studies have been made on positive columns. It is found that, when the two electrodes are brought together, the cathode dark space and negative glow are unaffected whilst the positive column shrinks. This process continues so that eventually the positive column, and then the Faraday dark space, are 'consumed', leaving only the negative glow and dark spaces adjacent to each electrode. This last situation is the usual case in glow discharge processes (Figure 4-3), where the inter-electrode separation is just a few times the cathode dark space thickness. The minimum separation is about twice the dark space thickness; at less than this, the dark space is distorted and then the discharge is extinguished.

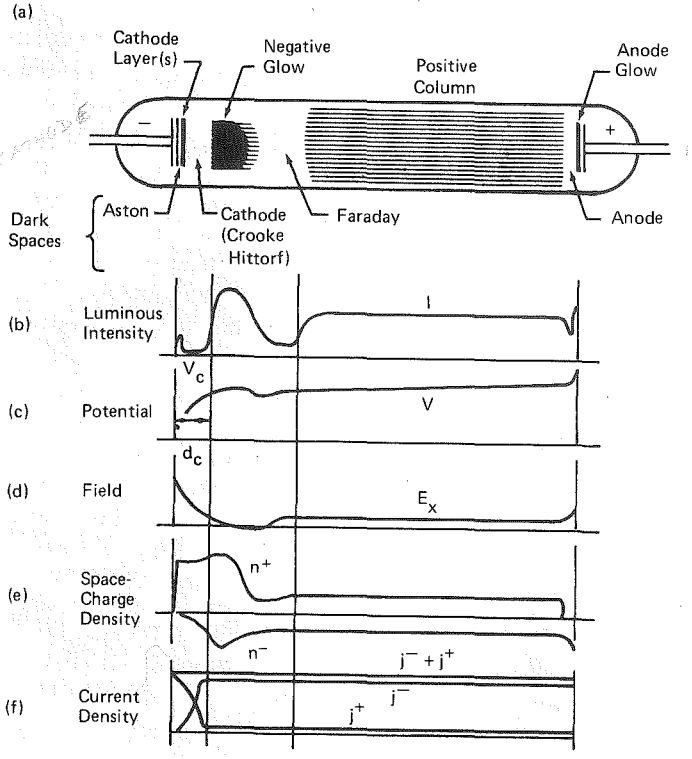

Figure 4-2. The normal glow discharge in neon in a 50 cm tube at p = 1 torr. The luminous regions are shown shaded (Nasser 1971). The abnormal glow would be somewhat different, although the glowing and dark regions would look the same

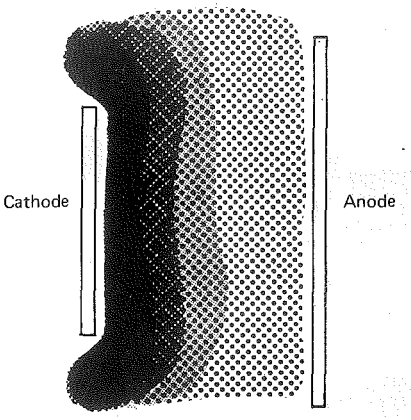

Figure 4-3. DC glow discharge process

Since current must be continuous in a system, it is clear that the currents at the two electrodes must be equal. In this particular system, the only other grounded electrode was remote from the discharge and had a small surface area; thus, the current densities at the chromium cathode and stainless steel anode were approximately equal. Take a typical datum point, which might be 2000V and 0.3 mA/cm^2 at 50 mtorr. This represents an electron current density to the anode that is much smaller than the random current density $\frac{1}{4}en\overline{c_e}$ and so there must be a net decelerating field for electrons approaching the anode, i.e. the plasma is more positive than the anode. But there is still some electron current flowing, so apparently the anode is more positive than floating potential. We earlier calculated a 'reasonable' floating potential 15V less than the plasma potential, and this is consistent with commonly found values of $V_p \sim +10V$ (with respect to a grounded anode) in dc sputtering systems.

The plasma is virtually field-free, as we saw earlier, so the plasma has the same potential V_p adjacent to the sheath at the cathode. But the cathode has a potential of -2000V, so the sheath voltage is $-(2000 + V_p)$, i.e. -2010V in our example (Figure 4-4).

Notice some peculiarities about this voltage distribution:

1. The plasma does *not* take a potential intermediate between those of the electrodes, as might first be expected. This is consistent with our earlier contention that the plasma is the most positive body in the discharge.
2. The electric fields in the system are restricted to sheaths at each of the electrodes.
3. The sheath fields are such as to repel electrons trying to reach either electrode.

All of these peculiarities follow from the mass of the electron being so much less than that of an ion. The third, in particular, is illustrative of the role played by electrons in a discharge.

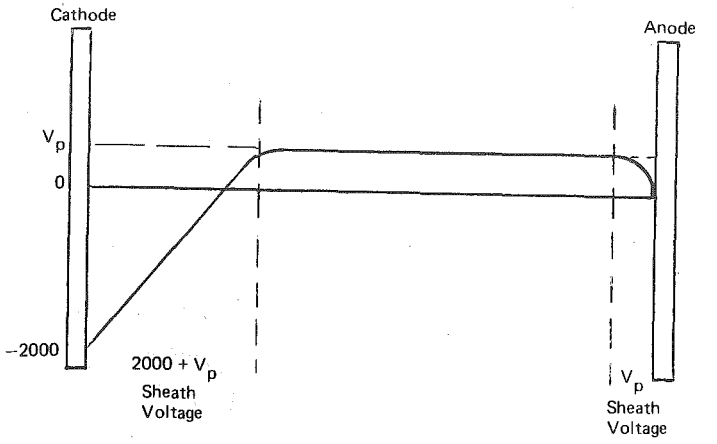

Figure 4-4. Voltage distribution in a dc glow discharge process

MAINTENANCE OF THE DISCHARGE

How is this glow discharge sustained? Electrons and ions are lost to each of the electrodes and to all other surfaces within the chamber. The loss processes include electron-ion recombination (which takes place primarily on the walls and anode due to energy and momentum conservation requirements, as we saw in Chapter 2), ion neutralization by Auger emission at the target, and an equivalent electron loss into the external circuit at the anode. To maintain a steady state discharge, there must be a numerically equal ion-electron pair generation rate; i.e. there must be a good deal of ionization going on in the discharge.

There is also a considerable energy loss from the discharge. Energetic particles impinge on the electrodes and walls of the system, resulting in heating there; this energy loss is then conducted away to the environment. So another requirement for maintaining the discharge is that there is a balancing energy input to the discharge.

How are these ionization and energy requirements satisfied? The simplest answer is that the applied electric field accelerates electrons, so that the electrons absorb energy from the field, and that the accelerated electrons acquire sufficient energy to ionize gas atoms. So the process becomes continuous. But that's a very simple answer, and raises various other questions. Where does most ionization take place, and what are the major processes involved? Can the model

of the discharge that we've been developing account for the amount of ionization required? To what extent is the dc discharge like the plasma of Chapter 3?

In trying to decide where most ionization occurs, the glow region must be an obvious candidate. In chapter 2, we saw that ionization and excitation are rather similar processes. Their thresholds and cross-section energy dependences are not so different, so that for electrons with energies well above threshold, ionization and excitation will be achieved in a rather constant ratio; as the electron energy decreases towards threshold, then excitation will occur in an increasing proportion since it has a lower threshold. So we would expect that excitation, and subsequent emission from de-excitation, will always accompany ionization – at least for the glow discharges we're considering. Hence the choice of the glow region as the prime candidate for the main ionization region. But if we look in the literature, then we often find descriptions of glow maintenance that rely entirely on ionization in the cathode sheath region. So apparently there is some disagreement over this matter.

In the rest of this chapter, we shall be examining a practical dc discharge in some more detail, and we shall do this by dividing the discharge into three regions: the cathode region, the glow itself, and the anode region. We shall be looking not only at the ionization question raised above, but also at practical matters such as charge exchange collisions in the sheath which have the important effect of controlling the energy of bombarding ions at the cathode – important in practical applications. But before looking at these three regions, we shall discuss the phenomenon of *secondary electron emission* that takes place at cathode, anode, and walls.

SECONDARY ELECTRON EMISSION

When a particle strikes a surface, one of the possible results is that an electron is ejected. The number of electrons ejected per incident particle is called the *secondary electron coefficient* or *yield*. Secondary electron emission is observed for bombardment by ions, electrons, photons and neutrals (both ground state and metastable); each will have a different coefficient and a different energy dependence.

Electron Bombardment

The emission of electrons due to electron impact has been closely studied because of its importance in valves, cathode ray tubes, and electron multipliers. By looking at the energy dependence of the emitted electrons (Figure 4-5), it appears that some of the bombarding electrons are elastically or inelastically scattered, and that some *'true' secondaries* are also emitted. The 'true' secondaries

are frequently, but not always, more numerous than the scattered primaries. Electron bombardment processes will be significant at the anode and at walls; there is no electron bombardment at the cathode. The yield due to electron impact is usually given the symbol δ, which depends on the energy of the bombarding electron, and is typically unity for clean metals (Figure 4-6). However,

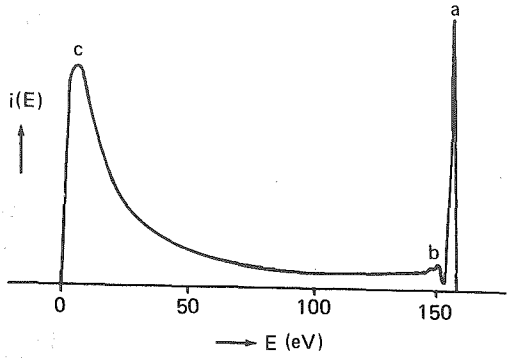

Figure 4-5. The energy distribution of secondary electrons emitted by silver (Rudberg 1930, 1934); a – elastically reflected primaries, b – inelastically reflected primaries, c – 'true' secondaries

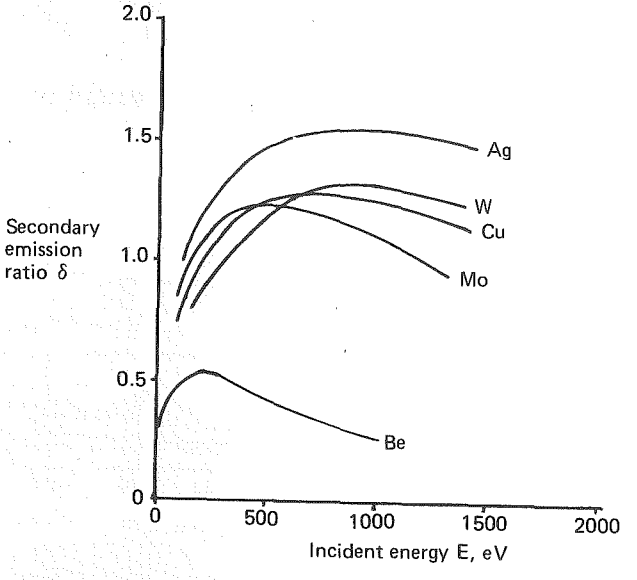

Figure 4-6. Secondary emission coefficient δ of different metals as a function of the energy of incident electrons (Hemenway et al. 1967)

δ is also strongly dependent on the presence of contamination or surface adsorbed layers, and is higher for insulating materials. Table 4-1 gives the maximum yield values δ_m and corresponding bombardment energies, and the *unity points* (one electron out for one electron in, therefore no net charging) for a number of materials. In glow discharge processes, we have to deal with electron bombardment at low energies of a few eV (and also some by high energy electrons – see later) so we would really like some δ data at correspondingly low energies, but it doesn't seem to be too readily available.

Ion Bombardment

The corresponding secondary electron emission coefficient for ion bombardment is given the symbol γ_i. Some values for γ_i are shown in Tables 4-2 and 4-3. The energy dependence of γ_i for noble gas ions on tungsten and molybdenum is shown in Figure 4-7, and for various other ion-metal combinations in Figure

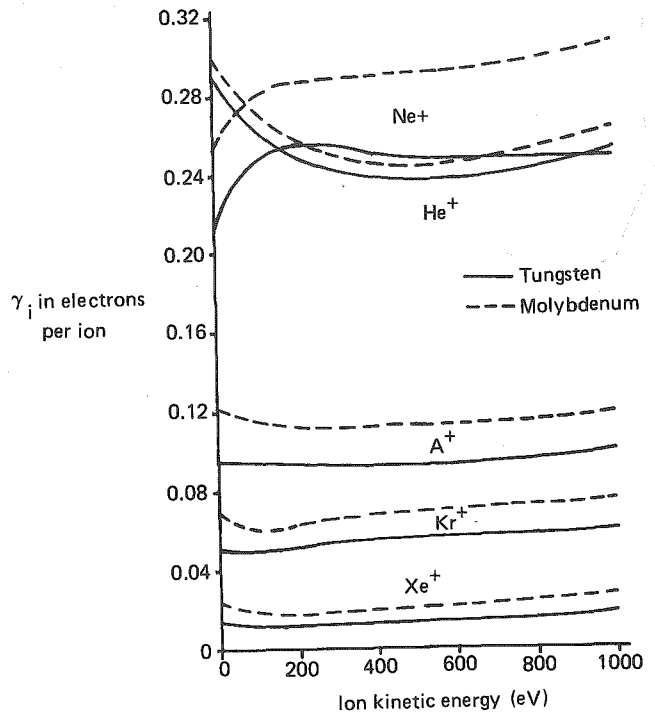

Figure 4-7. Secondary electron yields γ_i for noble gas ions on atomically clean tungsten and molybdenum (Hagstrum 1956b)

Table 4-1 Secondary Electron Emission Coefficients δ

	$\delta = 1$ at			
	V eV	V′ eV	δ_{max}	Energy (eV) for δ_{max}
Ag			1.5	800
Al			1.0	300
Au			1.5	800
C	160	~ 1000	1.3	600
Cu	> 100		1.3	600
Fe			1.3	350
Ge			1.1	400
K			0.7	200
Li			0.5	85
Mo	140	1200	1.3	350
Na			0.8	300
Pt			1.6	800
Pt			1.8	800
Pt	150	> 2000	1.8	800
Si			1.1	250
W			1.5	500
Zn	100	400	1.1	200
NaCl			6	600
NaCl	~ 20	1400	6–7	600
MgO (vacuum cleaved)			21	1100
MgO			2.4–4	400
MgO	< 100	> 5000	7.2	1100
Pyrex glass	30–50	2400	2.3	300–400
Soda glass	30–50	900	~ 3	300
Oxide cathode BaOSrO	40–60	3500	5–12	1400
ZnS		6000–9000		
Ca tungstate		3000–5000		

Two and three different sets of data (independent sources) are shown for Pt, NaCl, and MgO with considerable disagreement in the case of MgO (Lye 1955, Von Engel 1965, and Johnson and McKay 1953, respectively)

Data From:

McKay 1948
Bruining 1954
Woods 1954
Hachenberg & Brauer 1959
Von Engel 1965
Dekker 1963
Lye 1955
Johnson and McKay 1953, 1954
Copeland 1931

Table 4-2 Secondary Electron Coeficients γ_i for Argon Ion Impact

	Ion Energy		
	10 eV	100 eV	1000 eV
Mo	0.122	0.115	0.118
W	0.096	0.095	0.099
Si (100)	0.024	0.027	0.039
Ni (111)	0.034	0.036	0.07
Ge (111)	0.032	0.037	0.047

Data From:
Hagstrum 1956a, 1956b, 1960
Takeishi & Hagstrum 1965
Carlston et al 1965

Table 4-3 Values of γ_i From Metals for Slow (Sic) Ions

Metal	Ar	H_2	Air	N_2	Ne	
Al	0.12	0.095	0.021	0.10	0.053	
Ba	0.14	.....	0.100	.....	0.14	
C	.....	0.014				
Cu	0.058	0.050	.....	0.025	0.066	
Fe	0.058	0.061	0.015	0.020	0.059	0.022
Hg	.....	0.008	0.020			
K	0.22	0.22	0.17	0.077	0.12	0.22
Mg	0.077	0.125	0.031	0.038	0.089	0.11
Ni	0.058	0.053	0.019	0.036	0.077	0.023
Pt	0.058	0.020	0.010	0.017	0.059	0.023
W	.....	.....	.....	.....	.....	0.045

From Knoll et al. (1935); reported in Cobine (1958)

4-8. The yield is again very dependent on the condition of the surface: Figure 4-9 shows how γ_i depends on the crystal face exposed and Figure 4-10 shows how the yield of polycrystalline tungsten decreases from the clean metal value on exposure to nitrogen, reaching a new quasi-steady state after about 10 minutes, coinciding with the completion of the first monolayer coverage of the nitrogen. (Note also in Figure 4-10 that the ion bombardment energy is only 10 eV, so that γ_i is still quite high in this case, even at such low ion energies). The effect of surface contamination is again shown in Figure 4-11, this time for argon ion bombardment of tungsten. Figure 4-12 shows similar effects due to other gas adsorptions on tantalum and platinum.

These variations of yield γ_i with surface condition are quite important in dc sputtering where the magnitude of the yield plays a role in determining the V-I characteristics of the discharge. A sputtering target is immediately contaminated on exposure to the atmosphere, commonly with the formation of an oxide surface layer on metal targets. When the target is subsequently sputtered, there is a period when the V-I characteristic is continuously changing as the surface layer is removed.

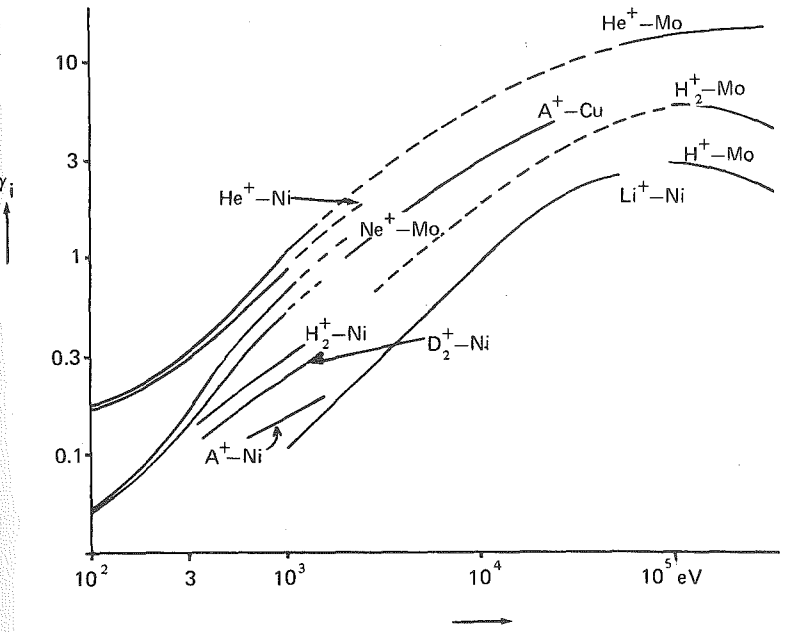

Figure 4-8. Secondary emission coefficient γ_i for ions of energy K falling on the surface of various substances, from von Engel (1965). References: Rostagni (1938), Healea and Houtermans (1940), Hill et al. (1939)

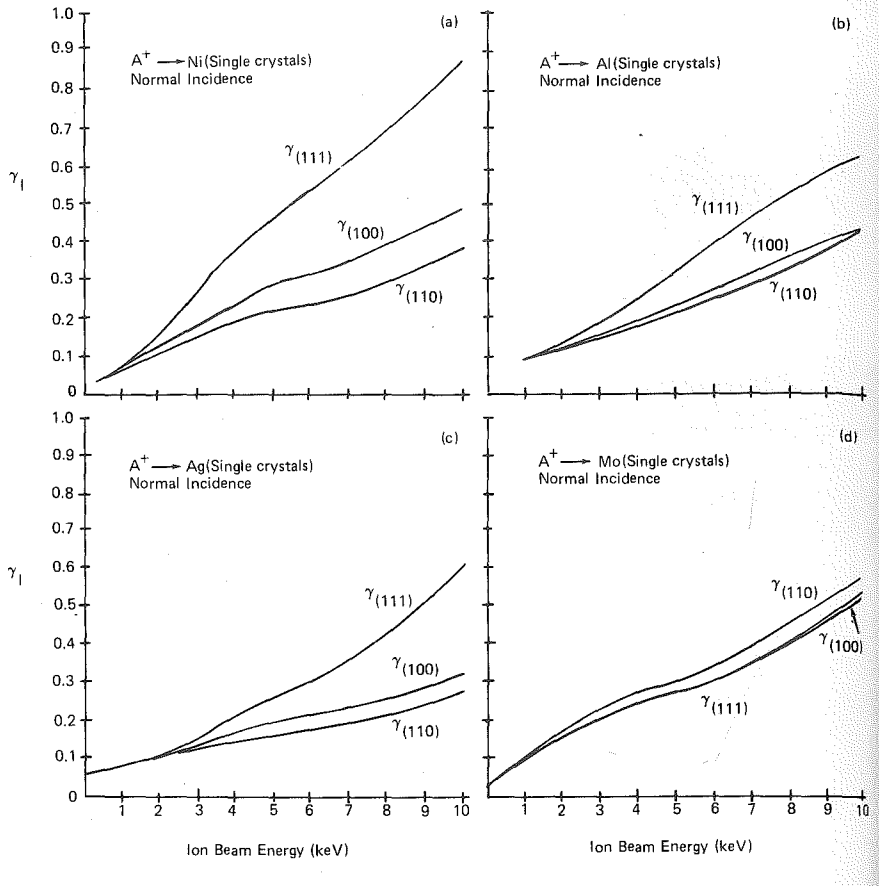

Figure 4-9. Variation of γ_i with ion energy for Ar^+ bombardment of (111), (100) and (110) surfaces of (a) nickel, (b) aluminium, (c) silver and (d) molybdenum (from Carlston et al. 1965)

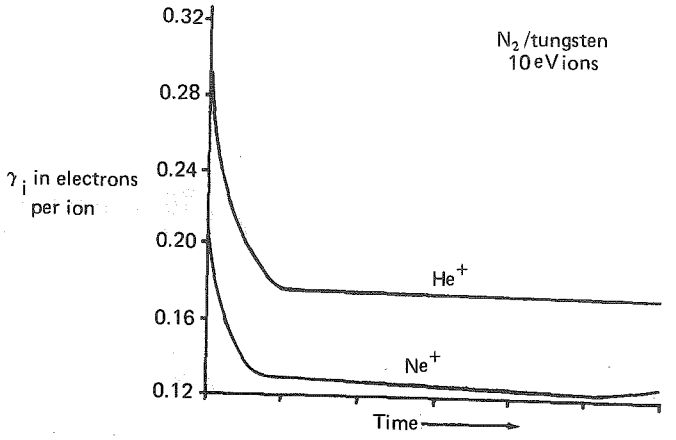

Figure 4-10. Secondary electron yields γ_i for He^+ and Ne^+ ions, as a monolayer of nitrogen forms on tungsten. The break in the plot represents the completion of the first monolayer (from Hagstrum 1956c)

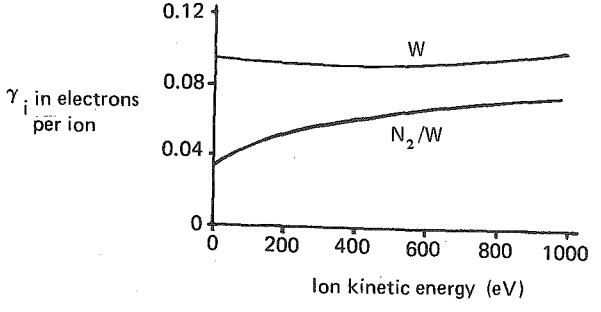

Figure 4-11. Secondary yield γ_i for argon ions on clean tungsten and on tungsten covered with a monolayer of nitrogen (from Hagstrum 1956c)

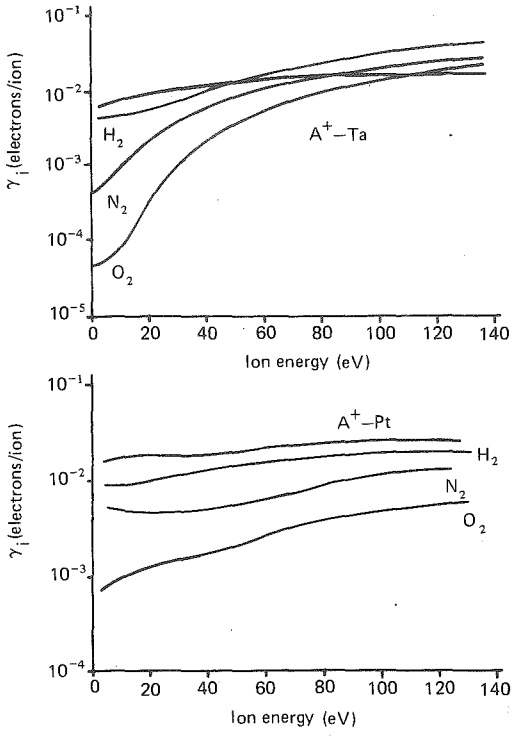

Figure 4-12. Secondary electron yields for Ar^+ ions on outgassed tantalum and platinum, and on these metals after treatment with hydrogen, nitrogen and oxygen (Parker 1954); n.b. logarithmic vertical axis. (From McDaniel 1964)

We have so far been dealing with pure metals having γ_i much less than unity. Insulators generally have much larger values, but there is a problem in obtaining accurate yield values due to the charging of the insulator. Some alloys also have large yields (Figure 4-13) which make them suitable for use as electron multipliers in dynode arrays.

We saw earlier that many of the secondary electrons emitted due to electron impact had rather low energies of a few eV. The same is true when the impacting particles are ions. Figure 4-14 shows the yields for various 40 eV noble gas ions. The dependence of the secondary electron energy distribution on the energy of the incident ion is rather weak (Figure 4-15), so that all emitted electrons have initial energies ~ 5 - 10 eV.

The interested reader is referred to McDaniel (1964), from which much of the data shown here has been taken, for a more thorough review of secondary electron emission due to ion impact.

In glow discharges, ion energies on targets and substrates range from a few eV up to a few hundred eV, and so the secondary electron yield data over the corresponding range are the most useful for the present investigation.

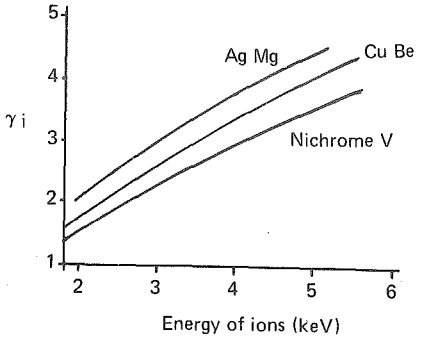

Figure 4-13. Electron yields for Ar^+ ions on Ag-Mg, Cu-Be and Nichrome V alloys (from Higatsberger et al. 1954)

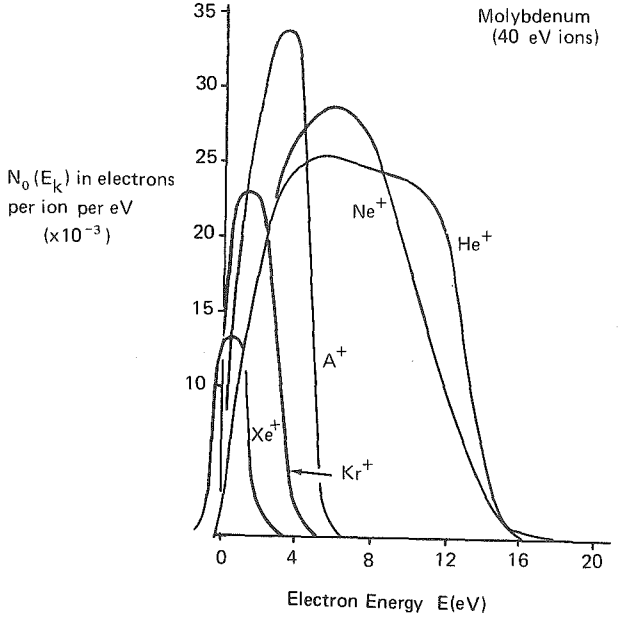

Figure 4-14. Energy distributions of secondary electrons ejected from Mo by 40 eV ions of the noble gases (Hagstrum 1956b)

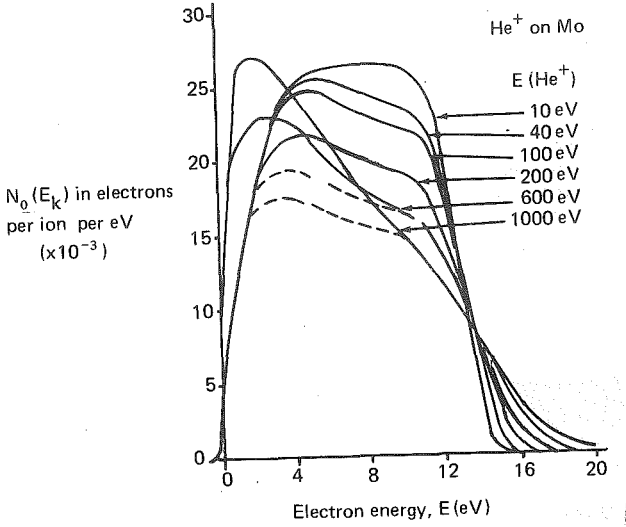

Figure 4-15. Energy distributions of secondary electrons ejected from Mo by He^+ ions of various energies (Hagstrum 1956b)

Neutral Bombardment

In the sheath at an electrode, energetic ions frequently collide with neutrals either elastically or with charge exchange (see Chapter 2) in either case giving rise to energetic neutrals. If sufficiently energetic, these neutrals can cause secondary electron emission. Figure 4-16 shows the yields for argon ions and argon neutrals on molybdenum. It appears that there is a potential energy component for the ions only. Unfortunately, there is rather little of this data available; Figure 4-16, if typical, suggests that electron emission due to neutrals is rather unimportant in glow discharge processes where neutral energies are a few hundred eV at most.

In Chapter 2, we saw that there are likely to be long-lived metastable neutrals, particularly in noble gas discharges. Although these metastables cannot be accelerated by electric fields, being neutral, they will receive energy by collision with energetic ions, the energy transfer function making this an efficient process. Since the metastables have some potential energy, they will presumably be somewhat more effective in producing secondary electrons than their corresponding ground state parents. There seems, however, to be rather little quantitative information available.

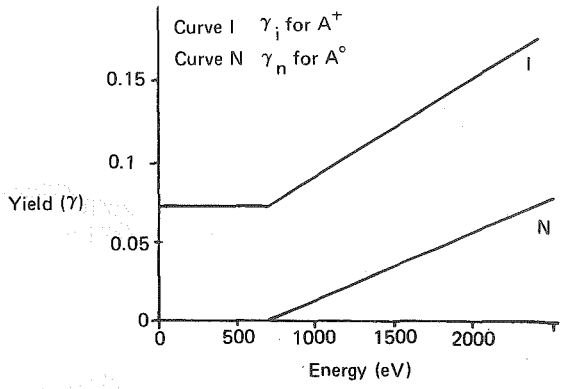

Figure 4-16. Secondary electron emission as a function of energy for argon ion and neutral atom bombardment of molybdenum (from Medved et al. 1963)

Photon Bombardment

The ejection of electrons due to photon bombardment is well-known, and is usually referred to as *photoemission*. For pure metals, the photoelectric yield γ_p depends on the work function ϕ of the metal, with a threshold for emission of $hc/\lambda = e\phi$. The photoelectric yields for most pure metals are only 10^{-4} to 10^{-3} electrons per photon in the visible to near ultraviolet frequencies, largely because the photon is usually efficiently reflected, except at very short wavelengths where a corresponding increase in photoelectric yield is seen, as in Figure 4-17. There doesn't seem to have been much consideration of the effect of photons in sputtering and plasma etching glow discharges. It does seem that, under the right circumstances, photoelectric yields can be as large as ion yields, and certainly there are believed to be strong photon effects in rather specific cases such as hollow cathode sources. Holmes and Cozens (1974) propose a contribution from photoelectric emission in their rather high current density mercury discharge (in which they also make the rather interesting observation of a pressure gradient near the target, believed to be due to the strong ion flux there). But on the whole, the effects of photoelectric emission and photoionization in glow discharges are not well understood.

Summary

Electrons can be emitted from solid surfaces due to the impact of ions, electrons, neutrals, and photons. Some of the processes are well understood, at least for clean metals. The situation for insulators and contaminated surfaces is much less

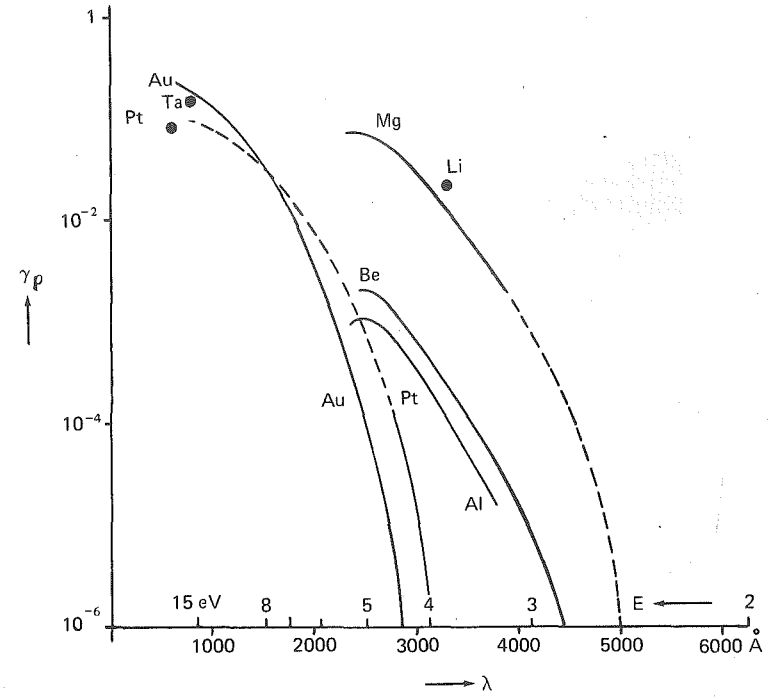

Figure 4-17. Photoelectric yield γ_p as a function of the wavelength λ of the incident light (energy E of quantum) for various substances (von Engel and Steenbeck 1932, Kenty 1933, Stebbins 1957, Wainfan et al. 1953). 2537 Å light yields $\gamma_p \sim 10^{-4}$ for borosilicate glass, 6 10^{-4} for soda glass; light of $\ll$ 1250 Å gives $\gamma_p \sim 10^{-3}$ for borosilicate glass (Rohatgi 1957). From von Engel (1965)

clear; experiments are complicated by the resultant charging of the surface. Harold Winters has pointed out to me that some of the literature on secondary electron emission, particularly the earlier literature and including some shown here, is likely to be erroneous, often because of the experimental difficulties encountered. For a discussion of modern measurement techniques, and an illustration of the importance of surface condition, see Sickafus (1977). Similar problems exist in measurements of both δ and γ. Theoretical considerations lead one to expect that γ will be independent of ion energy below 500 eV; the incoming ion is neutralized by an electron from the target, which then may Auger-emit another electron, so that the potential energy of the ion is important rather than its kinetic energy. This explanation is consistent with some of the data shown. The data of Hagstrum and colleagues is well regarded.

These processes are important in glow discharge processes because each of them can contribute electrons to the discharge and help to counter electron loss processes. Since the plasma is more positive than the potential of any surface in the discharge, the action of the sheath is to accelerate electrons from the surface into the glow, giving both electrons and energy to the discharge.

Our practical processes result in surface bombardment energies from a few eV up to several hundred eV or even a few thousand eV and we need, therefore, to consider secondary electron data over this range. Ion bombardment will clearly be of importance at the cathode of a dc discharge, and both electron and ion bombardment at the anode. The importance of metastable and ground state neutrals, and of photons, has to be further assessed.

The detail of the loss processes for electrons and ions at electrodes and walls is complicated by secondary electron emission from those surfaces. When we have previously looked at currents to surfaces, e.g. in "Sheath Formation at a Floating Substrate" in Chapter 3, we have tacitly ignored the effects of secondary emission, which would change the net current to a surface or modify its floating potential, for example.

THE CATHODE REGION

The type of dc discharge used in glow discharge processes is known as an *abnormal glow discharge*. At lower applied voltages and consequent lower currents, a discharge can result which is characterized by constant voltage and constant current density. This is a *normal glow discharge*. More power applied to the system is manifested by an increase in the size of the region of the cathode carrying current (j and V remaining constant) until the whole cathode is utilised, at which stage the discharge becomes abnormal. We shall not consider normal discharges further in this book.

The cathode plays an important part in dc sputtering systems because the sputtering target actually becomes the cathode of the sputtering discharge. The cathode is also the source of secondary electrons, as we have seen, and these secondary electrons have a significant role both in maintaining the discharge and in influencing the growth of sputtered films.

When the formation of sheaths was being considered in Chapter 3, we made the assumption that there were no collisions in the sheath. Many books and papers on plasma physics are concerned specifically with *collisionless plasmas*, but this is because most current interest is in plasmas which have very high temperatures of many keV, and these are essentially collisionless; such plasmas are of interest in fusion. 'Our' plasmas are very different and do have lots of collisions, both in the sheaths and in the glow. In a moment we shall look at some of these collision processes.

As already pointed out, in trying to understand the mechanisms by which a discharge is sustained, it is clearly necessary to account for all the recombination and energy loss processes which occur (Figure 4-18). We could simplify the situation for analysis purposes by considering a discharge between very large electrodes close together, which is usually the case in high pressure planar diode plasma etchers (see Chapter 7) and some sputter deposition systems (see Chapter 6). Unfortunately I don't have any quantitative data for this dc situation, but the data in Figure 4-1 should be reasonably representative.

To return to our example in "Architecture of the Discharge", a current density of 0.3 mA/cm^2 means that net currents of 1.9 10^{15} ions/cm^2 and 1.9 10^{15} electrons/cm^2 are flowing each second to the cathode and anode respectively. The ion flux at the anode should also be about 1.9 10^{15}/cm^2 sec, as we discussed in Chapter 3. So if we ignore the small electron current at the cathode due to secondary electron emission, and ion-electron recombination at the walls and in the gas volume, then we need an ion-electron pair production rate of at least 3.8 10^{15} ions per second for each cylinder of discharge emanating perpendicularly from the cathode and having 1 cm^2 cross-sectional area.

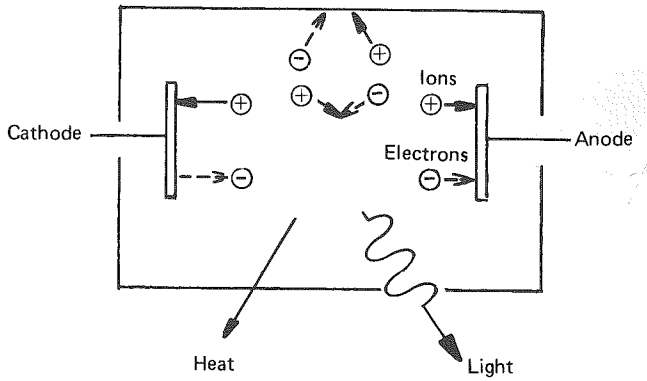

Figure 4-18. Discharge loss processes

Ionization In The Sheath

Electron Impact Ionization

Some descriptions of the glow discharge process rely on ionization caused by secondary electrons from the target as they are accelerated across the dark space (Figure 4-19). This can be modelled by considering the amount of ionization

caused by a flux $N_e(x)$ electrons passing through a thin slab of thickness Δx located x from the cathode (Figure 4-20). The density of neutrals is n and the ionization cross-section (assumed energy-independent for simplicity) is q.

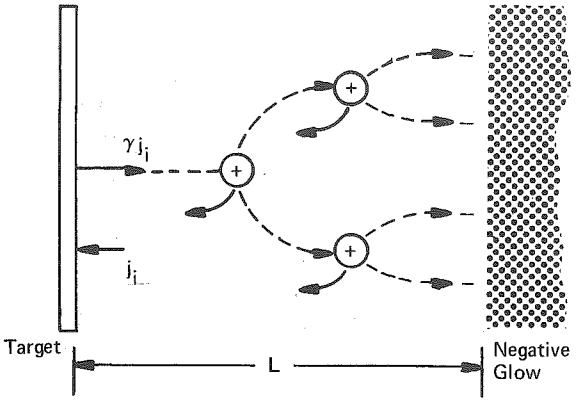

Figure 4-19. Ion pair production in the dark space

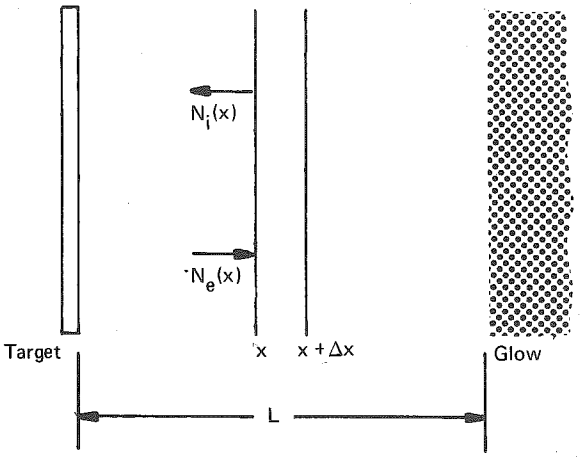

Figure 4-20. Analysis of ion pair production in the dark space

Number of ionizing collisions = $N_e(x)nq\,\Delta x$

$$\therefore \frac{dN_e(x)}{dx}\Delta x = N_e(x)nq\,\Delta x$$

$$\therefore \int \frac{dN_e}{N_e} = \int nq\,dx$$

$$\therefore N_e(x) = N_e(O)\exp nqx$$

So each electron that leaves the target is multiplied by exp nqL by the time it reaches the edge of the dark space. The electric field in this region is strong enough that the major part of the electron travel will be straight across the dark space along the field lines.

Let's obtain an idea of the magnitude of this electron multiplication for the practical conditions under consideration. In Chapter 2, "Ionization", we found that the maximum ionization cross-section for electrons in argon is $2.9\ 10^{-16}$ cm^2 for 100 eV. Davis and Vanderslice (1963), whose work on collisions in the sheath we shall be considering shortly, found a sheath thickness of 1.3 cm for a discharge voltage of 600V in argon at 60 mtorr, for which $n = 2.1\ 10^{15}$, using a Kovar alloy cathode. These figures put an upper limit on electron multiplication of exp $(2.1\ 10^{15} \times 2.9\ 10^{-16} \times 1.3) = 2.2$.

For each ionization, a new ion is formed as well as a new electron. For each electron that leaves the target, (exp nqL - 1) ions will be formed. For each ion that strikes the target, γ secondary electrons will be emitted, where γ is the sum yield for all of the various processes (see "Secondary Electron Emission"). Hence, each ion that strikes the target will lead to the generation of γ(exp nqL - 1) ions within the dark space. The yield γ is unlikely to exceed 0.2 for most metals, and this suggests an ion production rate of 0.24 ions per ion; remember that this is an upper limit based on the use of the maximum cross-section for ionization in argon.

Ion Impact Ionization

There may be other ionization mechanisms in the sheath. In Chapter 2, we saw that photoionization and ion impact on neutrals were both possible ionization mechanisms. I don't know the photon fluxes to be able to assess photoionization, although these could presumably be obtained with optical emission spectroscopy. But we can make an estimate of ion impact ionization. In the same way that we estimated electron impact ionization earlier, we can use the exp nqL expression to estimate ion impact ionization. Using the same example, n will be $2.1\ 10^{15}$ cm^3 and L will be 1.3 cm, as before. From Figure 2-25 (Chapter 2), we find a cross-section q of about $5\ 10^{-17}$ cm^2 for ions with mean energies of a hundred eV or so. So the ion multiplication factor will be about exp

$(2.1\ 10^{15} \times 5\ 10^{-17} \times 1.3) = 1.15$. Since secondary electron effects were ignored in Figure 2-25, this will be an overestimate (as was our earlier value for electron impact ionization). We therefore have an ion production rate by this process of 0.15 ions per ion compared with an equivalent of 0.24 ions per ion for electron impact ionization; although the electron cross-section is larger, there are fewer electrons. Both are maximum possible values, not actual; in reality, the contributions may be much smaller, particularly from the ions.

Sheath Ionization — Conclusion

An ion production rate of 1 ion per ion in the sheath would be adequate to maintain the ion flux to the cathode. But according to our analysis, this would be achieved by electron impact ionization only if L = 2.9 cm (for $\gamma = 0.2$) or L = 3.9 cm (for $\gamma = 0.1$), and there would not be such errors in the measurement of L. A production rate of 1 ion per ion would also be achieved, for the given value of nqL, if $\gamma = 0.8$. This also is unlikely, although it is true that our working figure of $\gamma = 0.1$ is based largely on ion impact secondary electron values, and we should add the effects of bombardment by fast neutrals, metastable and photons, so $\gamma = 0.8$ isn't out of the question. On the other hand, the q value we used was the maximum possible, and so values for ion production would be considerable overestimates.

Our finding of a certain amount of ionization by ion impact does not really change the situation since the maximum possible ion multiplication by this means was only 1.14.

Our general conclusion is therefore that there is some ionization in the sheath, but very probably not enough to maintain the ion flux to the target. In the next two sections on "Charge Exchange in the Sheath" and "Generation of Fast Electrons", we shall present some further experimental evidence to add credence to this conclusion, so that although none of the evidence presented is really conclusive by itself, the overall weight of evidence is quite convincing.

The inadequacy of sheath ionization becomes even further apparent when we remember that a similar amount of ionization is required to account for the ion current to the anode. Ions produced in the cathode sheath certainly cannot travel to the anode because of the polarity of the cathode sheath field. So we need a large source of ionization in either the negative glow or in the anode sheath. But the latter is so much thinner than the cathode sheath that any significant amount of ionization there is immediately ruled out. Which leaves the glow.

Charge Exchange in the Sheath

An ion arriving at the interface between the glow and a sheath has a kinetic energy that is negligible compared with most sheath voltages (see Chapter 3, "Sheath Formation and the Bohm Criterion"). In the absence of collisions, the

ion would accelerate across the sheath, losing potential energy as it does so, and would hit the electrode with an energy equivalent to the sheath voltage. But the ion usually does collide, with or without the exchange of charge (Figure 4-21) (see Chapter 2, "Ion-Neutral Collisions"). This effect is important in glow discharge processes because it modifies the energy distributions of particles striking the electrodes and substrate.

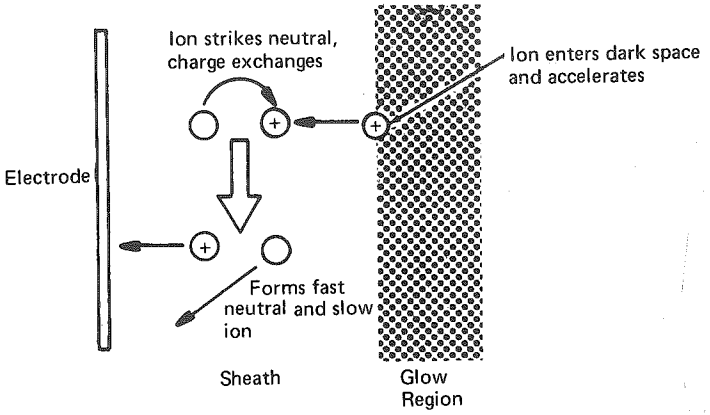

Figure 4-21. Charge exchange in an electrode sheath

Studies of the energy distributions of ions striking an electrode have been made by a number of authors; the work most relevant to glow discharge processes is by Davis and Vanderslice (1963). The apparatus they used is shown in Figure 4-22. Some of the ions striking the cathode pass through a tiny hole into a much lower pressure region where they are energy analyzed and then mass analyzed. The energy distribution of ions striking the cathode would be influenced not only by charge exchange but also by ionizing collisions in the sheath, and so could give us information about the latter. The results obtained by Davis and Vanderslice for Ar^+ ions in an argon discharge are shown in Figure 4-23; these results are consistent with their model which is based on the following assumptions:

1. All ions originate in the negative glow or very close to it. The model assumes little or no ionization in the sheath, and then uses the predictions of the model to test this assumption.
2. The dominant collision process is of symmetrical charge transfer ($Ar^+ + Ar \rightarrow Ar + Ar^+$) with the new ion formed starting at rest, and then accelerating

in the sheath field. There is no net change in ion flux, which therefore remains constant across the sheath.

3. The charge exchange cross-section is independent of energy, which is an approximation over the range used.
4. The electric field across the sheath decreases linearly to zero at the dark space – negative glow interface.

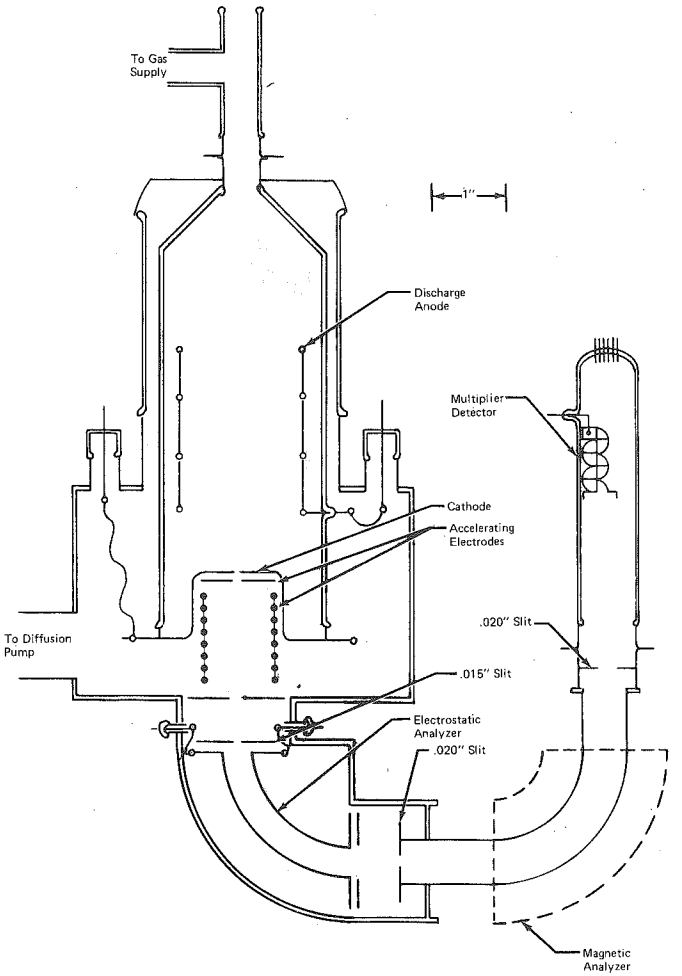

Figure 4-22. Experimental apparatus for the energy and mass analysis of ions bombarding the cathode in a dc discharge (Davis and Vanderslice 1963)

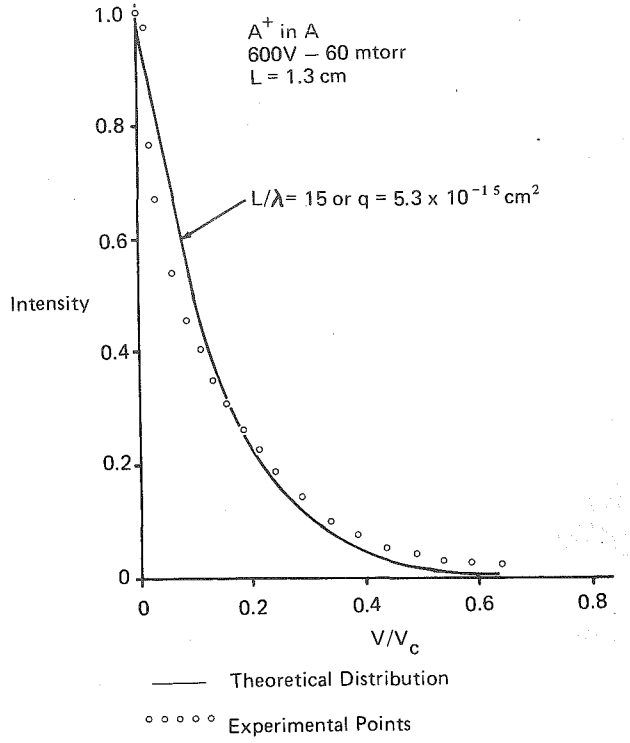

Figure 4-23. Energy distribution for Ar^+ from an argon discharge (Davis and Vanderslice 1963)

Using these assumptions and the parameters shown in Figure 4-24, Davis and Vanderslice obtained the theoretical distribution

$$\frac{V_c}{N_o}\frac{dN}{dV} = \frac{L}{2\lambda}\left(1 - \frac{V}{V_c}\right)^{-\frac{1}{2}} \exp - \frac{L}{\lambda}\left[1 - \left(1 - \frac{V}{V_c}\right)^{\frac{1}{2}}\right]$$

where V_c is the target voltage, and dN is the number of ions arriving with energies between eV and eV + edV; L is the dark space thickness and λ is the charge exchange mean free path. When $\lambda \ll L$, this distribution function reduces to

$$\frac{V_c}{N_o}\frac{dN}{dV} = \frac{L}{2\lambda} \exp\left(-\frac{L}{2\lambda}\frac{V}{V_c}\right)$$

The result for argon shows reasonable agreement with this model; in Figure 4-23, the open circles are experimental results and the solid line is a best fit from the

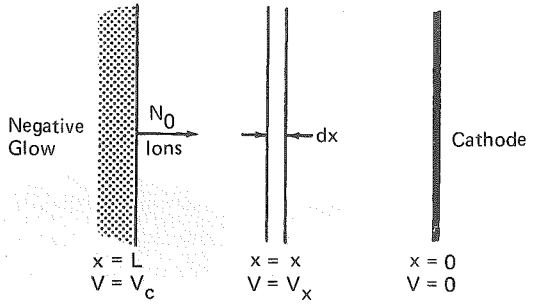

Figure 4-24. Model used to derive energy distributions (Davis and Vanderslice 1963)

theoretical expression, giving a cross-section of 5.3 10^{-15} cm^2 in reasonable agreement with other published values. Note that:

- The effect of gas pressure on the energy distribution is found to be small, if the discharge voltage is held constant. This is a result of the pressure – dark space thickness product being fairly constant for a dc discharge, so that the average number of collisions per ion in traversing this distance is reasonably constant.
- Increasing the target voltage (at constant pressure) causes the dark space to decrease in thickness, so that a relatively larger proportion of high energy ions will reach the cathode.
- Reduction of the collision cross-section also causes a larger proportion of high energy ions. Figure 4-25 is for A^{++} ions in argon, where a significant number of A^{++} ions (cross-section 7 10^{-16} cm^2) apparently traverse the sheath without collision.

The results of Davis and Vanderslice, which are confirmed by the later experiments of Houston and Uhl (1971), are used to illustrate the effect of charge exchange in limiting the energy of ion bombardment at the cathode. The good agreement between the theoretical and experimental results is also taken as confirmation that there is little or no ionization in the sheath.

However, I wonder how much of this agreement is fortuitous. Certainly there should be some ionization in the sheath, as we showed in the previous section, and this should have an effect on the energy distribution by generating ions in the sheath. Another questionable assumption in the Davis and Vanderslice model is that of a linear field variation in the sheath. From Poisson's equation, we know that such a variation is synonymous with uniform net positive space charge in the sheath; if $d\mathscr{E}/dx$ is proportional to x, then $\rho/\epsilon_o = d^2\mathscr{E}/dx^2$ = constant. Several authors refer to findings of linear field variations in the sheath.

Apparently the original findings are due to Aston (1911) who observed the deflection of a beam of electrons fired across the sheath. There are also some comments of findings of departures from linearity towards both interfaces of the sheath. If all ionization was in the glow, and ions entering the sheath were then accelerated freely, the ion density would decrease towards the cathode. The effect would be greatest in a collisionless sheath, and would be reduced by charge exchange collisions. If a linear field existed in the sheath, the potential would vary as x^2. Ingold (1978) has pointed out that, in practice, the potential variations of $x^{4/3}$ and $x^{3/2}$ given by the free-fall and high pressure versions, respectively, of the Child-Langmuir space charge equation (see "Space Charge Limited Current") are similar enough that they might be interpreted as a linear field variation. So it may be that the experimental evidence for the linear field is not accurate enough to differentiate between the various possibilities; alternatively the results obtained may not apply to our discharges.

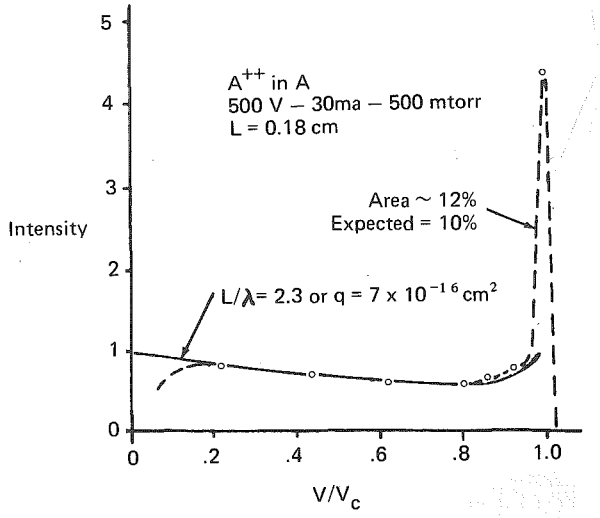

Figure 4-25. Energy distribution for Ar^{++} from an argon discharge. Dashed line and circles are experimental values while full line is the calculated distribution for L/λ = 2.3. The area of the peak represents those ions with the full cathode fall potential (Davis and Vanderslice 1963)

Generation Of Fast Electrons

If the secondary electrons emitted from the cathode were accelerated across the cathode sheath without making any collisions, then they would reach the edge of the sheath and enter the negative glow with an energy equivalent to the voltage drop across the sheath (give or take the energy of emission, and the sheath edge potential due to the Bohm criterion). Conversely, collisions in the sheath, including ionizing collisions, would attenuate this energy and also introduce a distribution of electron energies.

Brewer and Westhaver (1937) examined the energy distribution of electrons passing through a perforation in an aluminium electrode. The electrons were then deflected by a magnetic field and observed by fluorescence on a suitable screen. When the anode was at the sheath-glow interface, there was no change in the spot size or shape indicating that the electrons were still monoenergetic. When the anode was moved back into the glow region, the spot on the screen started to lengthen, implying electron energy inhomogeneity.

Voltages of 400 V to 30 000 V were used in these experiments. For 1000 V electrons, it was estimated that a change of 100 V could be readily detected. The conclusion was that less than 2 ions per electron were formed in the sheath. Although not specifically stated, it was implied that nitrogen was used for this work at pressures between about 0.1 - 4 torr.

It is not clear in Brewer and Westhaver's paper whether they used their technique to measure the actual energies of the electrons or only to measure the energy spread. It is also unclear how they moved their anode to the sheath-glow interface without grossly perturbing the discharge. Finally, I wonder how the motion of electrons was affected by the travel from the anode slit to the fluorescent screen 9 cm away, since there is no indication that differential pumping was used to reduce the pressure and eliminate collisions in this region.

In another group of experiments described in the same paper, Brewer and Westhaver measured the length of the negative glow (their discharge could be up to 40 cm long, unlike our applied discharges) for discharges in helium, hydrogen, argon and nitrogen. They obtained very good agreement with a theory of Lehmann (1927) for the range of fast electrons from the sheath, with the implication that the glow resulted from these fast electrons. Brewer and Westhaver again concluded that a large number, if not most, of the electrons entering the glow had an energy corresponding to the voltage across the sheath.

These experiments are further evidence that there is not a great deal of ionization in the sheath. However, they have a further and more practical significance: the fast electrons entering the glow have quite a small cross-section due to their velocity (as was seen in Chapter 2, and is rationalized in "The Glow Region") and as a result a significant number of these electrons hit the anode with sub-

stantial energies. In Chapter 6, "Life on the Substrate", we shall present experimental evidence for this phenomenon, which applies to rf as well as dc discharges, and see how it can influence thin film growth in a sputtering system.

Space Charge Limited Current

We still have some inconsistencies to eliminate. One of these is that the cathode sheath length in the examples earlier in this chapter was about 1 cm, which is typical of the values found, whereas earlier we had calculated sheath thicknesses characterized by a Debye length of the order of 100 μm.

Before we can remove this inconsistency, we need to understand the phenomenon of *space charge limited current*. We shall see that this does apply to the sheath regions of glow discharges, but we shall initially introduce the idea in relation to the emission of electrons from a heated filament in high vacuum, for simplicity.

Collisionless Motion

Figure 4-26 shows a heated wire filament emitting electrons to a positively biased anode distance d away. In Chapter 6, "Some Other Sputtering Configurations", we shall see how such *hot filament systems* are used for both sputtering and plasma etching applications. But in the present illustration, high vacuum is used to avoid ionization and thus restrict the system to a single charge carrier – the electron. The electron emission from a heated filament is given by the Richardson-Dushman equation:

$$j = AT^2 \exp - \frac{e\phi}{kT}$$

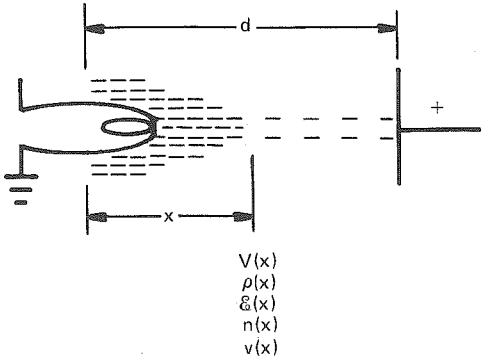

Figure 4-26. Space charge limited current from a heated filament

where ϕ is the *work function* of the filament material and A is a constant. In practice this value is not usually attained because an electron leaving the filament meets the strong Coulomb repulsion of the electrons which left previously, i.e. the actual emission current is limited by the space charge of the electrons. The limitation is overcome to some extent by applying an electric field to move the electrons away from the filament and reduce the space charge there.

At x (Figure 4-26), let the potential, electric field, electron density, electron velocity be V, ℰ, n_e and v respectively, where each is a function of x. Assuming a constant cross-section of the electron flux, j will be constant across the gap; m is the mass of the charge carrier, in this case the electron. For a single carrier:

$$j = nev \tag{1}$$

To find v, then by energy conservation

$$\tfrac{1}{2} mv^2 = eV$$

$$\therefore \quad v = \left(\frac{2eV}{m}\right)^{\frac{1}{2}} \tag{2}$$

To find n, then by Poisson's equation

$$\frac{d^2V}{dx^2} = -\frac{\rho}{\epsilon_0} = \frac{ne}{\epsilon_0}$$

This cannot be integrated directly because n is a function of x. But using equations (1) and (2) to express n in terms of V,

$$\frac{d^2V}{dx^2} = \frac{j}{\epsilon_0}\left(\frac{m}{2e}\right)^{\frac{1}{2}} V^{-\frac{1}{2}}$$

$$\therefore \frac{dV}{dx}\frac{d^2V}{dx^2} = \frac{j}{\epsilon_0}\left(\frac{m}{2e}\right)^{\frac{1}{2}} V^{-\frac{1}{2}} \frac{dV}{dx}$$

Integrating,

$$\frac{1}{2}\left(\frac{dV}{dx}\right)^2 = \frac{j}{\epsilon_0}\left(\frac{m}{2e}\right)^{\frac{1}{2}} 2V^{\frac{1}{2}}$$

The integration constant is removed since, if more electrons are being emitted than manage to reach the electrode, then the field is about zero at x = 0 (depending on the emission velocity of the electrons). Rearranging this and integrating once more,

$$V^{-1/4}dV = \left(\frac{4j}{\epsilon_0}\right)^{1/2}\left(\frac{m}{2e}\right)^{1/4} dx$$

$$\frac{4}{3}V^{3/4} = \left(\frac{4j}{\epsilon_0}\right)^{1/2}\left(\frac{m}{2e}\right)^{1/4} x$$

Again the integration constant is eliminated since $V = 0$ at $x = 0$. This equation is put into its more usual form by squaring and rearranging:

$$j = \frac{4\epsilon_0}{9}\left(\frac{2e}{m}\right)^{1/2}\frac{V^{3/2}}{x^2}$$

Note also that $V \propto x^{4/3}$, so that $\mathscr{E} = dV/dx \propto x^{1/3}$. This is the high vacuum version of the *Child-Langmuir* space charge limited current equation. It applies for all values of x, including d, the full extent of the voltage sheath. Note that it applies to a single charge carrier under collisionless conditions, so that the energy conservation equation can be used. It can clearly be used for any charge carrier by suitable choice of m.

In our example of thermionic emission, by increasing the voltage V we would eventually reach the saturation current limitation imposed by the Richardson-Dushman equation. Current could be increased further only by raising the filament temperature, as shown in Figure 4-27. So space charge limitation applies only in the absence of a more stringent limitation such as the supply of charge carriers.

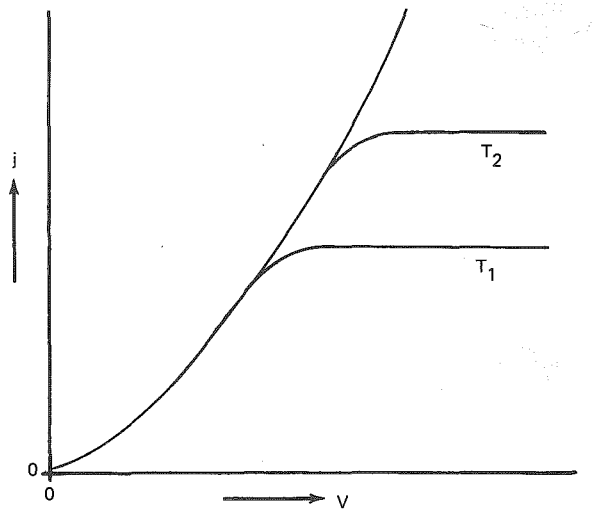

Figure 4-27. Space charge limited electron emission current versus voltage for two filament temperatures $T_2 > T_1$

Mobility Limited Motion

An electron travelling through a metal makes so many collisions that its *drift velocity* is quite small compared with its thermal velocity. We say that it is *mobility limited*. The drift velocity is proportional to the electric field; the constant of proportionality is the *mobility* μ, which we have already encountered in Chapter 3, "Ambipolar Diffusion".

To some extent, the same concept can be applied to gases, particularly in situations where the motion of the charge carriers is dominated by collisions. We can derive a space charge limited current equation for this case too, by substituting the drift velocity $V = \mu\mathscr{E}$ for the carriers instead of the velocity acquired by free fall. We would expect the resulting current to be smaller than for collisionless travel since it is now more difficult for the charge carriers to accelerate. Using a similar derivation,

$$j = nev = ne\mu\mathscr{E}$$

$$\frac{d^2V}{dx^2} = \frac{d\mathscr{E}}{dx} = \frac{ne}{\epsilon_0}$$

$$= \frac{j}{\mu\epsilon_0}\frac{1}{\mathscr{E}}$$

$$\therefore \tfrac{1}{2}\mathscr{E}^2 = \frac{jx}{\mu\epsilon_0}$$

$$\mathscr{E} = \left(\frac{2jx}{\mu\epsilon_0}\right)^{1/2} = \frac{dV}{dx}$$

$$\therefore V = \frac{2}{3}\left(\frac{2j}{\epsilon_0\mu}\right)^{1/2} x^{3/2}$$

and

$$j = \frac{9\epsilon_0}{8}\frac{V^2}{x^3}$$

This is the mobility limited version of the Child-Langmuir equation, sometimes known as the high pressure version, though somewhat misleadingly. Note that $V \propto x^{3/2}$, so that $\mathscr{E} \propto x^{1/2}$.

Application to Glow Discharge Sheaths

Which one of these space charge limited current equations apply to the sheaths in our discharges, if either?

The first problem is that the equations were derived for single charge carriers, and we have two – electrons and ions (and even more if multiple ions are included). Actually this isn't much of a problem because the electrons accelerate away from the sheath so rapidly that they produce a very small space charge density. However, this assumption of negligible electron density would not be true if there were copious ionization in the sheath.

Let's see what order of current densities are predicted by the two space charge equations. We'll use again the example from the data of Davis and Vanderslice – a 600 V sheath of thickness 1.3 cm, in argon so that m is 6.6 10^{-26} kg. Substituting these values into the collisionless Child-Langmuir equation, we obtain a value of 75 $\mu A/cm^2$. This seems quite low, at the bottom end of the values obtained in sputtering systems. But 600 V is quite a low cathode voltage for a dc sputtering system. Unfortunately Davis and Vanderslice do not report the current they obtained for this condition, but they do for another situation – 30 mA current from a 500 V sheath of thickness 0.18 cm at 500 mtorr. For these conditions the high vacuum current would be 2.9 mA/cm^2; since their target was 4.5 cm diameter, their actual current density was 1.9 mA/cm^2. The difference could well have been due to the charge exchange collisions in the sheath.

To use another example, Güntherschulze (1930) reports values for a helium discharge with an iron cathode, equivalent to a dark space thickness of 0.64 cm at 1 torr for a voltage of 1000 V. The high vacuum space charge density should then be equal to 2.1 mA/cm^2, which compares very well with the measured value of 2 mA/cm^2. The good agreement may be fortuitous, although the charge exchange cross-section for He^+ in He is several times lower than the equivalent figure for argon. And returning to argon, we should note that a 1000V sheath of thickness 1 cm would give a current density of 0.27 mA/cm^2; all of these values are consistent with observed sputtering values. We cannot expect to achieve very precise values of the space charge limited current because of the difficulties involved in assessing L, as will become more apparent in the next section. However, it does seem that the observed cathode currents are almost as large as the values predicted by the collisionless Child-Langmuir equation. This implies either that the saturation value of ion current from the glow has not been reached, or that the sheath thickness adjusts itself to extract precisely the saturation current. It would be difficult to test this in a diode discharge because increasing the cathode voltage would increase the power input to the discharge. The high voltage probe characteristics might be more illuminating. Tisone and Cruzan (1975) have measured the target voltage and sheath thickness for a target immersed in a hot filament discharge (see Chapter 6). They obtained rather good agreement with a $V \propto x^{4/3}$ relationship. It seems as though the sheath thickness is determined by the ion production rate in the glow and by the space charge limitation, at least in this case.

A second implication of the small differences between the free fall current limit and the measured values is that there are not many collisional processes in the sheath involving ions. This is further evidence that there is not much ionization in the sheath.

By definition, any motion in the sheath that is not free-fall is mobility limited, though not generally with the simple field-independent mobility μ assumed in the derivation of the mobility limited space charge equation. In Appendix 4, there are several sets of data relating to the drift velocity and mobility of ions and electrons in argon. You can see that these are plotted against $\mathscr{E}/p$. This is common practice when looking at conduction in gases at lower fields and higher pressures; even then μ is very dependent on $\mathscr{E}$, as can be seen from the data presented. Note that $\mathscr{E}/p$ is typically around a few volts/cm torr in these examples (although up to 100 and 240 volts/cm torr in two untypical cases). By comparison, our earlier example of a 500 V sheath of thickness 0.18 cm at 500 millitorr corresponds to $\mathscr{E}/p$ values increasing from about 0 at the sheath-glow interface up to 11 100 V/cm torr at the cathode, if we follow the assumptions of Davis and Vanderslice. Obviously we can 'predict' the observed values by suitably choosing μ, which in this example would need to be 446 cm^2/volt sec. If we guess, from Figure 4-23, at an average argon ion arrival energy at the cathode of 100 eV, then this is equivalent to a velocity of 2.1 10^6 cm/sec. The field at the cathode in this example is predicted to be 5.6 10^3 V/cm, so this gives a crude estimate of μ equal to 375 cm^2/volt sec. Mobility figures obtained in these two ways are virtually forced to agree, but the consistency is encouraging. The main point, however, is that these mobility figures are more than two orders of magnitude higher than equivalent figures obtained for conventional mobility limited situations. We can therefore conclude that ion motion in the sheaths of our dc discharges is much closer to free fall than conventional mobility limitation.

Finally, we should note that since the product of sheath thickness and pressure in dc systems is observed to be constant, then reducing the operating pressure will not significantly change the number of collisions in the sheath. By the same token, neither will increasing the pressure, and ion motion will remain closer to free-fall that mobility limited. Hence the earlier comment that the title of 'high pressure space charge equation' for the mobility limited situation was rather misleading. We can change the situation in rf systems which retain sheath thicknesses of about 1 cm even when the pressure is reduced down to 1 millitorr. At such a low pressure, collisions in the sheath become very unlikely and motion becomes essentially free-fall, albeit modulated by the applied rf.

Structure of the Cathode Sheath

We are now ready to account for the large difference between the Debye length and typical cathode sheath dimensions.

The Debye length was introduced in Chapter 3 by considering the space charge sheath formed around a perturbation in the discharge. In the subsequent derivation of the potential distribution around the perturbation, we assumed that the ion density remained constant at its unperturbed value. But as we have just seen, a large semi-permanent negative potential causes the formation of a positive space charge sheath of varying density. This sheath may be as much as a few cm thick. Our final sheath model (Figure 4-28) therefore has 3 regions:

- a quasi-neutral 'pre-sheath' in which ions are accelerated to satisfy the Bohm criterion, as discussed in Chapter 3.
- a region of the extent of a few Debye lengths in which the electron density rapidly becomes negligible.
- a region of space charge limited current flow, which would be of zero electron density in the absence of secondary electron emission from the target, and in practice is not so different because of the rapid acceleration of the electrons.

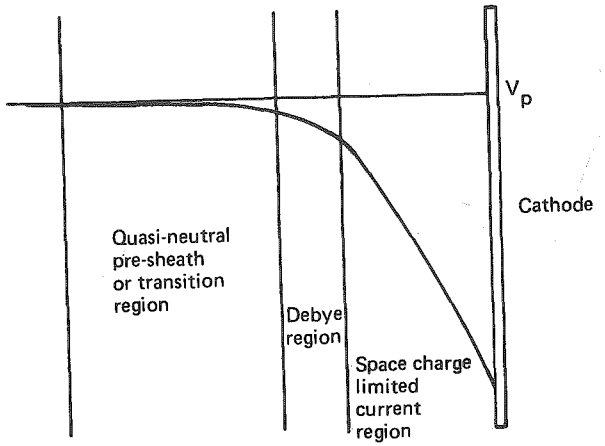

Figure 4-28. Regions of a cathode sheath

Of course, these divisions are in our minds only. A difficulty in experiments on sheath thicknesses is of trying to decide where the edge of the sheath is. Practically, people generally look for the change of luminous intensity due to de-excitation, either with a travelling microscope or an emission spectrometer with spatial resolution. But a change in intensity need not necessarily coincide with

the boundary of the sheath as we have defined it. Fortunately, since the average thermal velocity of excited atoms will be about 5 10^4 cm/sec, at least we don't generally have to worry about atoms moving appreciably between excitation and relaxation, which might not be the case for excited ions in the sheath or excited sputtered atoms, which have greater than thermal energies.

THE ANODE REGION

Structure of the Anode Sheath

In Chapter 3, we saw how a small sheath must be set up in front of the anode, of sufficient magnitude to repel some of the random flux $\frac{1}{4} n_e \overline{c_e}$ of electrons and reduce the current density at the anode to a more practical value. Our model of the sheath was essentially the same as that in front of a floating substrate (Chapter 3, "Sheath Formation at a Floating Substrate") except that the sheath voltage isn't as large at the anode. Later in Chapter 3, we needed to involve a pre-sheath or transition region to satisfy the Bohm criterion, and we expect this to apply to the anode too. The anode sheath is found to be so thin, usually about an order of magnitude less than the cathode sheath, that it should be essentially collisionless – and in particular not a source of ionization, which was tenuous even in the much thicker cathode sheath.

The anode sheath won't be very different from that in our derivation of Debye shielding. The Bohm criterion requires the ions to enter the sheath with an energy of about kT_e/e, and they then accelerate through the anode sheath to reach energies of 10 - 15 eV. The energy increase of a factor of 3 - 10 is equivalent to a velocity increase of $\sqrt{3}$ - $\sqrt{10}$, and an inverse change in ion density. The main point is that the ion density is not far from the uniform density assumed in the Debye sheath derivation, and does not vary anywhere near as much as in the cathode sheath. At the same time, the sheath voltage is small enough that the electron density does not go to zero as in the cathode sheath. The net result is that the anode sheath consists primarily of a pre-sheath and a Debye-like region.

Secondary Electron Emission

Unlike our simple model, in reality there is secondary electron emission from the anode. With the usual polarity of the anode sheath, these electrons are accelerated back into the glow, acting as a source of both electrons and energy to the glow. The anode is bombarded by ions, photons and electrons. Most of these come from the glow, except for the fast electrons which are generated in the cathode sheath; many of these travel through the glow without making many

collisions and strike the anode with considerable energy. These fast electrons are responsible for a significant power input to the anode.

As well as the fast electrons, there are slower electrons from the glow. The coefficient δ for electron bombardment tends to be larger than the coefficient γ_i for ion bombardment, so there are a significant number of electrons emitted and injected back into the glow, where we expect them to have an effect on the generation of the glow. Gillery (1978) has observed a considerable change in the V - I characteristics of his glow as substrates pass in front of his sputtering target. There is the implication in his work that it is the fast secondaries from the target which are having the greatest effect.

Note that another effect of secondary electron emission is to invalidate our earlier calculations of floating potentials and anode sheath potentials, which are therefore only approximately correct.

Space Charge Limited Anode Current

In our earlier attempts to consider the effect of space charge in limiting current flow, we were able to assume that there was a single charge carrier, or at least reasonably so. But in the anode sheath, the electron density is not necessarily insignificant, particularly if secondary electron emission from the anode is included. Therefore our existing collisionless form of the Child-Langmuir equation appears to be inadequate for the anode sheath, and a two carrier model is required. Testing of a model would be difficult since sheath voltage and thickness would both be small and subject to measurement error.

Polarity of the Anode Sheath

I have so far argued that the polarity of the anode sheath is such that the plasma potential will always be more positive than the anode. This is not always the case. Two reasons for the polarity would be

- high secondary electron coefficient at the anode
- physically small anode.

To treat the first of these, suppose that the electron and ion fluxes to an anode are j_e and j_i respectively. If the secondary electron coefficient for electron bombardment is δ, and if we add together the effects of ions and photons so that the secondary electron flux due to these bombardments is γj_i, then the net electron flux to the surface will be $j_e - (\delta j_e + j_i + \gamma j_i)$. Clearly this expression would be negative for values of $\delta > 1$. Of course the actual net current must be an electron current. The discharge achieves this by reducing the anode sheath voltage so that j_e (and also δj_e) increases. By continuing this process, the sheath voltage reduces and then *changes polarity*. At this stage j_e has reached its random value and no

longer increases, whilst the ions encounter a retarding field at the anode so that j_i decreases; the ejected secondary electrons now encounter a repulsive force so that the less energetic of the δj_e and γj_i electrons return to the anode. It would be interesting to run a discharge using an anode with a large δ to assess the practical extent of this sheath field reversal.

A second reason for polarity change at the anode sheath is anode size. For a given discharge of given total current, the current density at the anode would have to increase as the anode size is decreased. This would be achieved by decreasing the voltage of the anode sheath so that fewer electrons are repelled. The electron current could increase in this way until it reaches saturation when the anode is at plasma potential. Further increases in net electron current are then achieved by reducing the ion current, i.e. the sheath polarity reverses.

Main Effects in the Anode Region

The polarity of the anode sheath is usually such as to accelerate secondary electrons from the anode back into the glow, and also to accelerate ions from the glow onto the anode and onto any substrate there. Although the sheath is too thin to be a likely source of ionization, the accelerated secondary electrons act as both an electron source and an energy source to the glow. The sheath has to rely on the glow as an ion source. Since there appears to be rather little ionization in the cathode sheath and even less in the anode sheath, the ion fluxes at each electrode are of similar magnitude.

THE GLOW REGION

And so we come to the glow region. Although the glow is an ionized gas of approximate charge neutrality, it certainly isn't the uniform isotropic plasma described in Chapter 3. The main reason for this is the beam of fast electrons entering the glow region from the cathode sheath; these penetrate into and through the sheath and make it very anisotropic. People refer to three groups of electrons in the glow:

- *primary electrons* which enter from the cathode sheath with high energy; the name is slightly confusing because these same electrons were secondary electrons emitted from the target.
- *secondary electrons* of considerably lower energy; these are the product electrons of ionizing collisions or primaries which have lost much of their energy.
- *ultimate electrons* which have become thermalized to the plasma temperature; these ultimate electrons have the highest density. In a low current density neon discharge at 1 torr, Francis (1956) reports densities of $5\ 10^6$, $5\ 10^7$, and $4\ 10^9$ for the primary, secondary, and ultimate electrons, respectively.

One might at first think that the primary electrons would soon lose their directionality and energy. However, as we saw in Chapter 2, there is a tendency for cross-sections to decrease with increasing energy at high energies. The rationale for this is illustrated in Appendix 4 for electron interactions; all interactions in plasmas are fundamentally electronic in nature. Another consequence of the weak interaction is that of *forward scattering*, i.e. the incident particles are not deflected much from their initial path.

So there is a good chance of fast electrons passing through the glow and colliding with the anode. We shall see experimental evidence for this in Chapter 6, in a sputtering application. Since the electron collision cross-section continues to decrease with increasing energy, there comes a point where increasing the voltage across a diode system has little effect – the electrons pass right through. This is the phenomenon of the *runaway electron*, and is encountered in very high temperature plasmas as an obstacle to heating (i.e. putting energy into) the plasma. This is not really a problem in our cold plasmas, although the seeds of the problem are evident.

In a long glow discharge, where there is room for a positive column to develop, then the energy of the primary electrons can be attenuated before they reach the positive column. As a result the positive column is much more like an idealized plasma, which has made it a popular testing ground for probe theories. The negative glow, with its three groups of electrons and anisotropic nature, is obviously a more difficult region to deal with. Some folks have used *directional probes* to try to distinguish between the various groups of electrons (Fataliev et al. 1939, Polin and Gvozdover 1938, Pringle and Farvis 1954), but there seem to be problems of interpretation. There are two-temperature models of the glow, pertaining to the secondary and ultimate groups of electrons, and probe measurements to substantiate a Maxwell-Boltzmann energy distribution for each of these groups. Ball (1972) has observed such two-temperature distributions in a dc sputtering discharge.

Ionization in the Negative Glow

In the next few sections we shall be considering the contributions of the various ionization mechanisms that can exist in the glow region. Remember that, using the example in "Architecture of the Discharge", we need an ionization rate of at least $3.8\ 10^{15}$ ions/second for each cm^2 of cathode to maintain an argon discharge of 0.3 mA/cm^2 at 2000V.

By Fast Electrons

The fast electrons entering the glow will obviously cause some ionization. Figure 2-8 shows the energy dependence of the ionization cross-section in argon. The

ionization rate will be nq per cm per electron. Although we should really consider the energy dependence of q, let's use an average value of $1.3\ 10^{-16}\ cm^2$, which is half of the maximum value and should be reasonable over the energy range considered. In contrast to the situation in the cathode sheath, we should not use the multiplicative (exponential) version of the ionization rate here because the electron produced by the ionization will have an energy of only a few eV. In the absence of the large field of the cathode sheath, this slow electron will not immediately produce further ionization.

Assuming a value of 0.1 for γ, the electron current at the edge of the glow will be 0.03 mA in our example, equivalent to an electron flux of $1.9\ 10^{14}$ electrons/cm^2 sec. At a pressure of 50 mtorr, the ionization rate per cm^3 per sec will be

$$1.9\ 10^{14}\ (3.54\ 10^{16} \times 50\ 10^{-3})\ 1.3\ 10^{-16},$$

which is $4.3\ 10^{13}$ ions/cm^3 sec. Even allowing for a glow length of 5 cm, this figure is too low, by a factor of at least 20, to sustain the discharge. This large difference could not be sensibly accounted for by underestimation of γ or of electron multiplication in the cathode sheath. So we conclude that the fast electrons do not directly cause enough ionization to sustain the glow.

By Thermal Electrons

Electrons just above threshold have a smaller ionization cross-section than the fast electrons from the cathode, so how can the slow electrons cause much ionization?

Figure 4-29 is an electron energy diagram of the discharge, redrawn from Figure 4-4. Assume that the electrons are thermalized with a Maxwell-Boltzmann distribution around the electron temperature T_e. Figure 4-29 tells us that an electron in the plasma needs an energy of eV_p to reach the anode and $e(2000 + V_p)$ to reach the cathode. The probability of the former is $\exp(-eV_p/kT_e)$, which has a small but finite value of $7\ 10^{-3}$ for $V_p = 10$ V and $kT_e = 2$ eV. The probability of the electron returning to the cathode is virtually zero – less than 10^{-99}, which is as far as my calculator goes! The net result is that electrons become trapped in the glow region, generally being reflected at the interfaces with the electrode sheaths, including the sheath at the wall, before eventually managing to overcome the anode barrier. So the effective path length is increased as necessary to maintain the ion and electron densities by electron impact ionization.

Let us see if the amount of ionization in the glow is adequate to maintain the glow. The temperature of the electrons in the glow is typically around 2 eV – 8 eV, which is not adequate to ionize argon, which has a first ionization potential of 15.7 eV. But of course, in a Maxwell-Boltzmann distribution, some particles

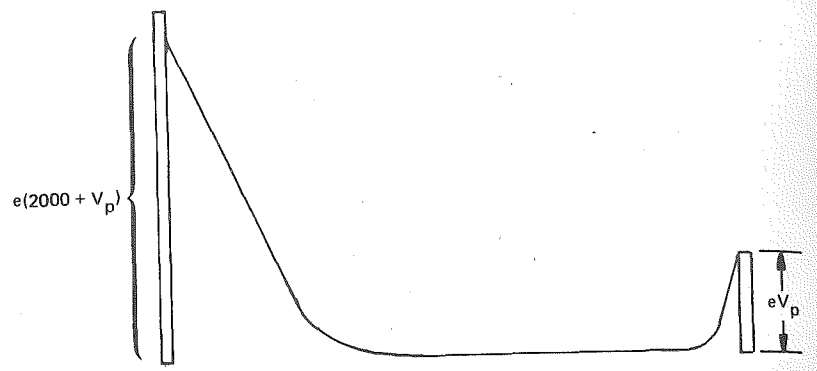

Figure 4-29. Electron energy diagram for the dc glow discharge

have energies far in excess of the mean. In Chapter 1, we saw that the speed distribution of such a gas is given by:

$$\frac{dn}{n} = 4\pi \left(\frac{m}{2\pi kT}\right)^{3/2} c^2 \exp \frac{-mc^2}{2kT} \, dc$$

Since the kinetic energy E can be written in terms of speed c as

$$E = \tfrac{1}{2} mc^2$$

then

$$c = \left(\frac{2E}{m}\right)^{1/2}$$

and so

$$dc = \tfrac{1}{2} \left(\frac{2E}{m}\right)^{-1/2} \frac{2dE}{m}$$

Hence we can derive an energy distribution:

$$\frac{dn}{n} = \frac{2}{\pi^{1/2}} \frac{1}{(kT)^{3/2}} E^{1/2} \exp - \frac{E}{kT} \, dE$$

perhaps more conveniently written as

$$\frac{dn}{n} = \frac{2}{\pi^{1/2}} \left(\frac{E}{kT}\right)^{1/2} \exp - \left(\frac{E}{kT}\right) d\left(\frac{E}{kT}\right)$$

This version of the Maxwell-Boltzmann distribution function tells us how the number of particles is distributed as a function of their energy E with respect to the temperature T of the distribution. The expression can be used in various

ways, for example to calculate the fraction f ($E > E_o$) of electrons in a Maxwellian distribution of temperature T_e, that have an energy greater than E_o:

$$f(E > E_o) = \frac{2}{\pi^{1/2}} \int_{E_o/kT_e}^{\infty} \left(\frac{E}{kT_e}\right)^{1/2} \exp\left(\frac{-E}{kT_e}\right) d\left(\frac{E}{kT_e}\right).$$

Some values obtained for this integral are shown in Table 4-4. The fraction of electrons which are energetic enough to excite argon (threshold 11.56 eV) or ionize argon (threshold 15.76 eV) are also calculated for a number of electron temperatures.

Table 4-4

The table shows the fraction f ($E > E_o$) of particles having an energy greater than E_o in a Maxwellian distribution of temperature T_e.

E_o	kT_e	E_o/kT_e	f ($E > E_o$)
		0	1.0
		0.5	$8.2\ 10^{-1}$
		1	$5.9\ 10^{-1}$
		2	$2.7\ 10^{-1}$
		3	$1.2\ 10^{-1}$
		4	$4.8\ 10^{-2}$
		5	$1.9\ 10^{-2}$
		7	$3.0\ 10^{-3}$
		10	$1.8\ 10^{-4}$
11.56 eV	0.25 eV	46.2	$7.0\ 10^{-20}$
argon	0.5	23.1	$5.4\ 10^{-10}$
excitation	1.0	11.6	$4.0\ 10^{-5}$
threshold	2.0	5.78	$9.5\ 10^{-3}$
	4.0	2.89	$1.3\ 10^{-1}$
	8.0	1.45	$4.2\ 10^{-1}$
15.76	0.25	63.0	$4.1\ 10^{-27}$
argon	0.5	31.5	$1.4\ 10^{-13}$
ionization	1.0	15.8	$6.9\ 10^{-7}$
threshold	2.0	7.88	$1.3\ 10^{-3}$
	4.0	3.94	$5.1\ 10^{-2}$
	8.0	1.97	$2.8\ 10^{-1}$

But this tells us only the proportion of electrons *capable* of ionization. We can calculate the *rate* of creation of ion-electron pairs by using the cross-section data referred to in Chapter 2. We saw that the cross-section q(E) was a function of energy. This cross-section, as defined earlier, gives an ion pair production rate nq(E) per electron per centimetre path length of the electron. For our present purposes, it is more useful to know the rate per unit time, i.e. in c centimetres at an electron speed of c. We can therefore write the rate of ion pair production per unit volume of the plasma per unit time as:

$$\text{Ion production rate} = \int_0^\infty n\, q(E)\, c\, dn_e(E)$$

since $dn_e(E)$ is the number of electrons having energies between E and E + dE, with corresponding speeds varying between c and c + dc, and n q(E) is the probability per unit length of forming an ion from a volume density n of gas atoms.

Examining the function within the integral, we know that q(E) is zero for all energies up to the ionization threshold eV_i. The integrand then begins to take nonzero values with q(e) monotonically increasing and $dn_e(E)$ monotonically decreasing. The cross-section q(E) can be written as a $(E - eV_i)^b\ \pi a_o^2$ for all values of E greater than the ionization threshold eV_i, by making a power curve fit to the data of Rapp and Englander-Golden (1965) discussed in Chapter 2. The speed term can be written as $(2E/m)^{1/2}$, and $dn_e(E)$ is just the Maxwell-Boltzmann distribution function. Since there is no ionization below the threshold, the integral becomes

$$\int_{eV_i}^\infty n\, a(E - eV_i)^b\ \pi a_o^2 \left(\frac{2E}{m}\right)^{1/2} n_e \frac{2}{\pi^{1/2}} \left(\frac{E}{kT_e}\right)^{1/2} \exp\left(\frac{-E}{kT_e}\right) \frac{1}{kT_e}\, dE$$

where

n = number/cc = p (torr) x $3.54\ 10^{16}$

a = 0.125 for argon

b = 1.077 for argon

E is in eV

eV_i = 15.7 eV for argon

$\pi a_o^2 = 8.82\ 10^{-17}$ cm^2

$\left(\frac{2E}{m}\right)^{1/2}$ is in cm/sec

$= E^{1/2}\ 5.93\ 10^7$ cm/sec, E in eV

n_e = plasma density/cc

$\frac{2}{\pi^{1/2}} = 1.13$

The integral is thus

$$2.09\ 10^8\ p\ a\ n_e \int_{\frac{eV_i}{kT_e}}^\infty (E - eV_i)^b\ E^{1/2} \left(\frac{E}{kT_e}\right)^{1/2} \exp\left(\frac{-E}{kT_e}\right)\ d\left(\frac{E}{kT_e}\right)$$

This can be evaluated numerically, for example with a programmable calculator, and some values thus obtained are shown in Table 4-5. For the sake of illustration, these are based on a plasma density of 10^{10}/cc in argon at 50 mtorr, but note that the ion pair production rate is proportional to both p and n_e, so that the corresponding rates under other conditions can readily be assessed. Interestingly, the proportion of electrons having a specific energy seems to decrease with energy at about the same rate as the cross-section increases. As a result, ionization is not confined to the group of electrons just above threshold, as one might at first guess.

Table 4-5 Ion Pair Production Rates in Argon

p = 50 mtorr, $n_e = 10^{10}$/cc.

kT_e	Production Rate (per cc per sec).
0.25 eV	$5.2\ 10^{-11}$
0.5	$3.5\ 10^{3}$
1.0	$3.7\ 10^{10}$
1.5	$9.2\ 10^{12}$
2.0	$1.6\ 10^{14}$
2.5	$9.0\ 10^{14}$
3.0	$3.0\ 10^{15}$
4.0	$1.4\ 10^{16}$ *
8.0	$2.0\ 10^{17}$ *

*These values are based on an integration up to 100 eV using the same power curve fit to the ionization cross-section data. The resulting values are too large, but by less than a factor of 2.

Remembering that the minimum ionization rate required to sustain our discharge is 3.8 10^{15} ions per sec per cm^2 of the target, then if the length of the glow in the example is 5 cm, this corresponds to an ionization rate of 7.6 10^{14}/ sec cm^3. From Table 4-5, this can apparently be achieved by a Maxwellian distribution of 10^{10} electrons/cm^3 with a temperature of 2.5 eV, which is a realistic figure for our discharges. And a small increase in electron temperature would provide enough ionization to account for wall losses, too. These calculations therefore suggest that the negative glow could provide enough ionization to sustain the discharge.

By Ions

One of the ionization mechanisms in the cathode sheath that we considered was of ionization by ion impact on neutrals, and it seemed as though there could be a small contribution. By contrast, the energy of ions in the glow will be very low, with an average ion temperature of less than 1000 K. And even for the very few ions with energies above the ionization threshold, the relevant cross-section will be much less than 10^{-18} cm^2, as can be seen in Figure 2-25. So ion impact can be completely ignored as an ionization source in the glow.

Of Metastables

A metastable argon atom has an excitation energy of 11.56 eV (or more) which is only 4.2 eV below the ionization energy. So the metastable can be ionized by a much larger proportion of the electrons in the glow than can a ground state atom. Since the metastable has already been excited by some energy input, this is known as a two step ionization process. Although there are many fewer metastables than ground state atoms, perhaps this is offset by the larger number of electrons which could ionize the metastables.

To make this calculation, we need to know the density of metastables and their ionization cross-section. Neither of these is well-known, so some guesswork is required. Eckstein et al. (1975) have measured the density of metastable neon atoms (16.62 eV and 16.72 eV) in a neon rf sputtering discharge at 20 mtorr, and found values of 10^{10} - 10^{11} cm^{-3}. We won't be wildly wrong if we guess at 10^{11} cm^{-3} for the argon metastables in our dc sputtering example. There is even less information about the ionization cross-section of the metastables, so let's assume that it has the same value as the maximum cross-section of 2.6 10^{-16} cm^2 for the ground state atom, but is energy independent above the threshold of 4.2 eV.

The rate of ionization by this process can be calculated in a similar way to that used for the ionization of ground state atoms. The technique that is shown in Appendix 4 can be used for any process with a constant cross-section

above a given threshold. Some rates of electron impact ionization of argon metastables, for the assumed values of n* and q and various conditions typical of the practical glow discharge, are shown in Table 4-6. If we then compare these values with the rates of ground state ionization at equivalent electron temperatures, we find that around 2 - 4 eV the ionization rate of metastables is smaller, but not much smaller. The apparent reversal of roles at low temperatures is primarily due to the assumption of constant metastable density. John Coburn has pointed out to me that the metastable atom might well have a much larger cross-section than its ground state partner; this could make the ionization of metastables comparable to that of ground states for electron temperatures of 2 - 4 eV, although it would still appear to be inadequate above 4 eV. We would be unwise, therefore, to ignore the ionization of metastables in the glow as a possible source of ion-electron pairs.

Table 4-6

Electron impact ionization of metastable argon atoms, assuming:

metastable density n*	10^{11} cm^{-3}
electron density n_e	10^{10} cm^{-3}
ionization cross-section q	2.6 10^{-16} cm^2
ionization threshold	4.2 eV

Electron Temperature	Ionization Rate per cm^3 per second
1.0	1.30 10^{12}
2.0	8.97 10^{12}
2.5	1.32 10^{13}
3.0	1.71 10^{13}
3.5	2.07 10^{13}
4.0	2.40 10^{13}
5.0	2.97 10^{13}
6.0	3.45 10^{13}
8.0	4.26 10^{13}

Summary

From the calculations in the last few sections, it appears as though the main source of ionization in the discharge is by electron impact ionization of ground state argon atoms in the negative glow, with possible additional contributions from electron impact ionization and ion impact ionization in the cathode sheath,

and from ionization of metastables in the glow. But these calculations were based on certain assumptions involving the electron distribution and the electron temperature, so let's examine those assumptions further.

The Electron Energy Distribution

We have been using the Maxwell-Boltzmann distribution to represent the energy distribution of electrons in the glow, or rather of those electrons that are not primary electrons from the cathode. The Maxwell-Boltzmann distribution applies to an assembly of particles in complete thermal equilibrium, for example the atoms in an ideal gas. By contrast, the electrons in the glow are in a non-equilibrium situation. The slower electrons make elastic collisions only, whereas electrons with energies above the excitation and ionization thresholds are liable to lose a large fraction of their energy by the corresponding inelastic processes. Fast electrons are also lost rapidly by diffusion to the walls, and recombination there. As a result, there is a transfer process of electrons from high energy to low energy states. So we might expect to have fewer electrons with high energies than the Maxwellian distribution predicts.

Druvestyn and Penning (1940) have tried to be more realistic by considering the motion of electrons in a weak electric field, such as that existing in the glow. The distribution which is so obtained, known as the *Druvestyn distribution*, when compared with a Maxwellian distribution predicts more electrons with energies around the average energy but many fewer electrons with energies greater than a few times average. However, their derivation still ignores inelastic collisions. Thornton (1967) has discussed how this model has been developed. Druvestyn and Penning (1940) and a later more detailed analysis by Holstein (1946), introduce a constant inelastic cross-section above threshold and this serves to further reduce the number of electrons with energies above threshold. Barbiere (1951) has included the velocity dependence of the elastic collision cross-section into his analysis. He shows that this has a very significant effect also in reducing the number of high energy electrons in argon because the Ramsauer effect causes the argon elastic collision cross-section to increase with increasing electron energy, in contrast to helium where it decreases.

The analyses above lead one to expect almost no energetic electrons at all. But experimentally the glow discharge electron distribution is found to be much more Maxwellian than it should be, based on these analyses. This is known as *Langmuir's Paradox*, and it was 30 years after Langmuir's original work that the resolution of the paradox began to be clarified, and I believe that the clarification is incomplete even now.

The analyses which produced this dilemma were based on the assumptions that the glow electrons gain their energy from the weak electric field across the glow, and that there is no energy interchange amongst the electrons. To treat the latter assumption, Thornton (1967) quotes the work of Dreicer (1960), who considered the effect of electron-electron and electron-ion interactions (see Appendix 4) on the electron distribution (actually in hydrogen gas). Dreicer concludes that these interactions can have a major effect in restoring the distribution to Maxwellian, but only at higher degrees of ionization ($> 10^{-2}$) than are encountered in our glow discharges ($\sim 10^{-4}$), so it still leaves us with a deficit of high energy electrons.

Any significant departure from a Maxwellian electron energy distribution will render invalid all the calculations we have made based on that distribution. In particular, it will enormously reduce the amount of ionization produced by the tail of the distribution in the glow and raise once again the question of how the glow is sustained.

In the rest of this chapter, I shall attempt to show that the main energy input to the electrons in the glow is from the fast electrons from the cathode rather than from the weak electric field across the glow, and that there are more energy interchange processes in the glow to be considered. An understanding of these sections is not essential before reading about the practical processes in Chapters 6 and 7, and a cursory reading may be adequate first time through.

Energy Dissipation in the Discharge

In order to clarify a couple of terms that I shall use, consider one of the 'water splash' rides that one sees at fairgrounds (Figure 4-30a). Having been mechanically raised, the boat accelerates rapidly down a ramp so that it acquires kinetic energy as it loses potential energy; let's say that a lot of kinetic energy is *generated* in the ramp. The boat then hits the water and is quickly slowed down as its energy is *dissipated* by transfer to the water. Note that no energy is generated in the water trough since it is level.

Let's see if we can apply some of these ideas to the discharge. There are three regions to consider: the sheaths at cathode and anode, and the glow itself. Using the values in our example again, we need at least $3.8\ 10^{15}$ ions produced per second per cm^2. Each ionization step requires a minimum energy of 15.7 eV, whether by one-step or two-step processes. The minimum energy consumption is therefore $3.8\ 10^{15} \times 15.7$ eV/sec cm^2, which is equal to $3.8\ 10^{15} \times 15.7 \times 1.6\ 10^{-19}$ joules/sec cm^2, or 9.6 mW/cm^2. In practice, the electron energy loss per ionization is more than 30 eV since the collision products also have some kinetic energy, and there will be many more ionizing collisions than $3.8\ 10^{15}$ / cm^2 sec to account for wall losses. There will also be further energy losses due to the inelastic collisions producing excitation. If, as seems likely, most ionization occurs in the glow, then the power consumption there (requiring an equiva-

lent amount of dissipation) will be at least 9.6 mW/cm^2, and probably several times this value. The glow region is rather like the water trough in the analogy, except that the glow does have some electric field across it. We have already seen that the glow should be equipotential within a few kT_e/e, and this appears to be consistent with measurement; Brewer and Westhaver (1937) found values of just a few volts. Let's assume 10 V across the glow. The current through the glow in our example is 0.3 mA per cm^2 of the target. These values give a power generation in the glow of 3 mW/cm^2, considerably less than even the very minimum value of 9.6 mW/cm^2 which must be dissipated there.

Where does this energy come from? The main power generation in the discharge is in the cathode sheath, and amounts to 2010 x 0.3 mW/cm^2, i.e. 603 mW/cm^2. Most of this goes into kinetic energy of ions and subsequently into heating of the cathode. We won't be far wrong by assuming a collisionless sheath and a secondary electron coefficient of $\gamma = 0{\cdot}1$, so that 10% of the current is carried by electrons. In the absence of collisions, these electrons enter the glow with a kinetic energy equivalent to the cathode sheath voltage, and so inject 60 mW/cm^2 of power into the glow, notably adequate to account for the ionization required with power to spare. The excess power is consistent with the observation that some fast electrons lose very little or no energy in the glow and hit the anode at high velocity. We shall see some evidence of this in Chapter 6, when we look at sputtering. It's as though the water trough in our analogy was not completely efficient in arresting the motion of the boats, so that some boats hit the end wall with considerable velocity even in the presence of a 'braking' hill (Figure 4-30b). I now understand my fear of such amusements! Notice the similarity between Figures 4-29 and 4-30b.

Energy Transfer Amongst the Discharge Electrons

The calculations and experimental evidence we have presented so far could be made consistent if the electrons from the sheath act as an energy source to the glow region. But how is this energy transferred?

Inelastic Collisions of Fast Electrons

Some of the fast electrons make ionizing collisions. As a result, they produce a second electron with a few eV of energy and also slow down due to the energy loss. Because of the energy dependence of the ionization cross-section, their propensity for further ionization increases. The deceleration of these electrons is increased because they also excite atoms, sometimes simultaneously with ionization. Of these processes, only the production of second electrons by ionization directly adds to the energy of the glow electrons. The photons resulting from ex-

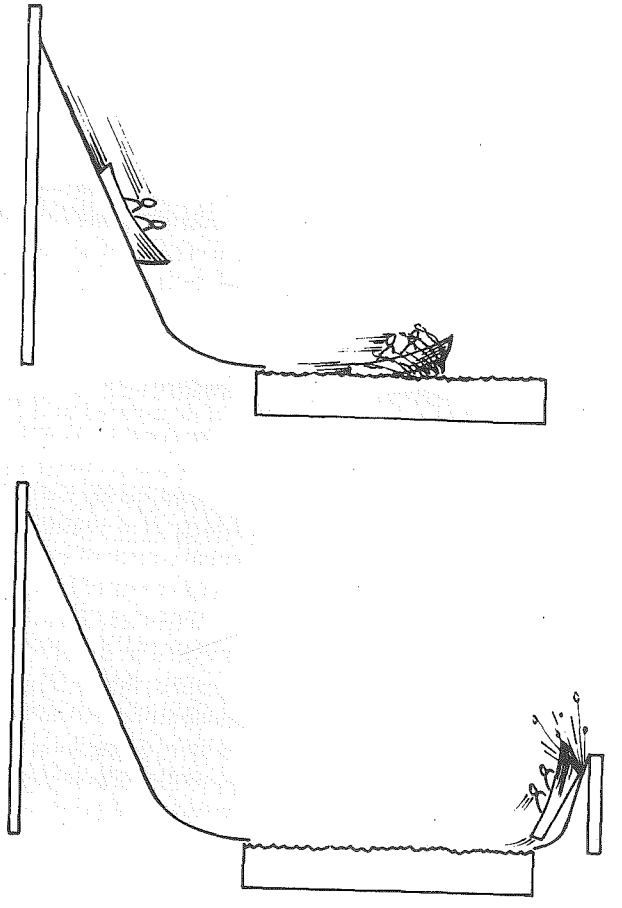

Figure 4-30. The water splash

citation probably don't do much in the gas phase because the cross-sections are too low, but they may cause secondary electron emission from the chamber walls.

In an earlier section on "Ionization in the Negative Glow", we calculated a rate of 4.3 10^{13} ionizing events per sec per cm travel of 0.03 mA of fast electrons entering the glow. Allowing a loss of 30 eV for each of these collisions, power dissipation in the glow will be 0.21 mW/cm^2 per cm length, or 1 mW/cm^2 if we include a glow length of 5 cm. This value is a significant addition to the com-

parable figure of 3 mW/cm^2 generated in the glow, but is still far short of requirements.

Note that the figure of 0.2 mW/cm^2 per cm is in good accord with the results of Brewer and Westhaver (1937) and Lehmann (1927). According to the latter, the range of 700 V electrons in argon at 1 torr is 5 cm, with an inverse dependence on pressure that would imply a range of 100 cm at 1 mtorr. A current of 0.03 mA at 700 V would have an initial energy of 21 mW, and if this is attenuated at a rate of 0.2 mW/cm, the resulting range would be close to 100 cm. On further thought, this is probably where the value of 30 eV per ionizing collision came from!

To return to the problem of transferring energy to the glow, the values we have obtained suggest the loss of energy by the fast electrons due to inelastic processes alone is inadequate to develop the power dissipation required in the glow.

Electron-Electron Collisions

We have already mentioned, in "The Electron Energy Distribution", the subject of electron-electron collisions. These are a potential source of energy exchange since the equal masses involved maximize the energy transfer function, and the Coulomb interaction between them is quite long-range, leading to a large effective cross-section. In principle, the cross-section would be infinite since the Coulomb interaction is, too. But we have to remember that in a plasma, the collective behaviour of electrons and ions causes electric fields to be *screened*, as discussed in Chapter 3 in connection with the Debye length λ_D. When we examine the electron-electron interactions in more detail, as in Appendix 4, we find a collision frequency of 1.3 10^5 per second, very comparable to the value of 4 10^5 per second for atom-atom collisions in an ideal gas, derived in Chapter 1, "Collision Frequency". However, the individual collisions are so weak that the energy transfer is insignificant for a 100 eV electron, amounting to only 2 10^{-4} eV/cm. The energy transfer is inversely proportional to the energy (see Appendix 4), but even for a 1 eV electron, the loss due to collisions with other electrons is only 1.4 10^{-2} eV/cm. On the other hand, the energy transfer is almost proportional to the electron density, so if the electron density were 10^{14} cm^{-3}, the transfer would be about 20 V/cm for a 10 eV electron, i.e. strong interaction, consistent with the results of Dreicer (1960) discussed in "The Electron Energy Distribution".

Interactions With Plasma Waves

The electron-electron collision analysis discussed above was based on the summation of individual pair interactions, and the analysis ignored any collective behaviour. Is this reasonable?

We have already briefly referred to some experiments by Langmuir (1925); he made some probe measurements on a *hot filament discharge*, in which electrons are thermionically emitted from a heated cathode and enable a discharge to be sustained with a few tens of volts. Using the probe technique discussed in Chapter 3, Langmuir identified three groups of electrons in the discharge:

- *primary electrons* from the cathode, which retain practically all the momentum acquired by acceleration across the cathode sheath, and hence are directional.
- *secondary electrons*, moving in random directions with a Maxwellian distribution about a temperature proportional to the primary beam energy (200 000 K for 100 eV primaries). This group includes primaries which have lost most of their energy and electrons emitted from ionizing collisions.
- *ultimate electrons*, which were the most numerous, ~ 10^3 times the density of the primaries and secondaries, with a Maxwellian distribution of energies around 1 - 3 eV. These were assumed to be secondary electrons which had lost most of their energy to join the ultimate group.

We have previously mentioned these three groups of electrons. What is more relevant in the present context is the energy spread of the primary electrons that Langmuir observed. At low discharge currents the electrons were quite monoenergetic with a spread of about 2 volts for a 50 V beam. However, when the current was raised, there were electrons with energies both greater and less than the interelectrode potential; for example, for a beam current of 10 mA, the primary beam energy was about 47 volts, with a spread of ± 10 V. Langmuir referred to this as the phenomenon of *high scattering*; Tonks and Langmuir (1929) subsequently found high frequency oscillations in the discharge – the *plasma oscillations* discussed in Chapter 3.

Langmuir's approach was refined, and the connection between high scattering and the oscillations established, by the experiments of Merrill and Webb (1939). They used an indirectly heated cathode to avoid magnetic field effects, and a probe which could be moved by very small increments. This enabled them to discover that, although oscillations existed everywhere, they had a sharp peak in the glow, in a very localized region a few tenths of a millimetre deep. The 'high scattering', observed as a velocity modulation about the initial primary electron energy, appeared in a distinctly separate region about 0.5 mm nearer to the cathode. The reason for these separate locations can now be understood in terms of the operation of a *klystron*. The modulation of the electron velocity in the region of high scattering introduces many different electron velocities, but does not change the current in that region. However, the faster electrons now begin to catch slower electrons so that the phenomenon of *electron bunching*

appears – for the same reason that public transport buses come in threes. The bunching is observed as oscillations in current (which is what the probe was looking for) and will reach a maximum some distance 'downstream' from the region of velocity modulation, as observed by Merrill and Webb. (In the klystron, velocity modulation of a beam of electrons is produced by applying a small high frequency voltage modulation via a resonant cavity. As a result, electron bunching occurs, and the current oscillations produced further down the beam are used, with a suitably placed second cavity, to induce a power modulation in an external impedance. The power delivered to the external impedance comes primarily from the kinetic energy of the electron beam, so that power amplification from the input modulation to the output modulation has occurred, i.e. the klystron is a high frequency amplifier).

In the klystron, and in the plasma too, the fast electrons do not overtake the slower electrons. This is because the bunching causes an increased negative space charge which repels and decelerates the fast electrons as they try to overtake the slower electrons. The net result is that the electrons in the beam vibrate about the positions they would have occupied in the unmodulated beam, at the plasma frequency, as discussed in Chapter 3; at the same time, the whole electron beam moves at the original velocity. So we have *space charge waves* moving through space.

Wehner (1950) turned Merrill and Webb's findings, in a somewhat different arrangement, into a practical device – the *plasma oscillator*. This oscillator is very much like a klystron, except that it uses the plasma itself to generate the oscillations rather than an external source.

An objection to the Merrill and Webb experiments was that the probe perturbed the plasma – the standard objection to probes. Cannara and Crawford (1965) carried out similar experiments on a hot filament discharge, using an electron beam rather than a probe. The thin beam is fired across the discharge, and the resulting deflection is used to determine the electric fields in the discharge. Their results essentially confirm the earlier work, and Cannara and Crawford conclude that the beam of electrons interacts with the plasma so strongly that the rf oscillations generated disperse the beam, in their experiments within about 1 cm for a beam of tens of electron volts energy, in a mercury discharge at 0.2 - 1.0 millitorr.

But we have still not explained *how* the primary electrons give up their energy to the glow electrons. The plasma waves have to be formed in the first place, and then they have to be persuaded to give up their energy. Bohm and Gross (1949, 1950) laid the foundations for solving these problems. Their papers show that if beams of sharply defined velocity or groups of particles with far above mean thermal speeds are present in a glow, such as the beam of electrons from the cathode sheath entering the glow, then there is a tendency towards instability

so that small oscillations grow. They then go on to show how electrons in the glow can be trapped by a plasma wave, so that the trapped electron is forced to run with the wave, oscillating back and forth in the potential trough of the wave, with an average velocity equal to the wave velocity. This is the phenomenon of *electron trapping*.

Chen (1974) compares this situation with that of a surfer trying to catch an ocean wave. At first the surfboard merely bobs up and down and does not gain energy. The surfer then 'catches' the wave, is accelerated and gains energy, whilst the wave loses energy and is damped. In the same way, the plasma wave can trap electrons until it is completely damped.

An initial requirement for the surfer, and for the glow electrons, is that their velocity is close enough to the wave velocity for them to become trapped, and so only a fraction of the electrons will be affected. But there are many waves in the plasma other than those due to the primary electrons, and these propagating plasma oscillations can have a whole range of velocities, so that the entire distribution of glow electrons can be affected by waves. If the surfboarder in the analogy were moving faster than the wave, he could give energy to it; so electrons moving faster than the wave can become trapped and give energy to the wave.

The analysis of Bohm and Gross has been well substantiated subsequently. Chen describes some experiments which demonstrate the existence of both standing and travelling electron waves, again using probes.

There are many other wave phenomena to consider, such as Landau damping, wave-wave interactions, and ion waves, but such considerations are beyond the scope of this book and, quite frankly, beyond me at the moment. However, it does appear that the wave-electron interaction may be capable of explaining both the attenuation of the primary electrons when they enter the glow, in order to slow the primary electrons as observed and to 'heat' the plasma, and to account for the energy interchanges tending to push the plasma back towards a Maxwellian distribution. I wonder also how far one can extend the comparison with the klystron and argue that the plasma is like a distributed detector and external impedance, so that the power of the oscillations is amplified by the primary beam energy and then dissipated in the glow impedance.

The energies of the primary electrons in our cold cathode discharges are very much higher than in the hot filament discharges used by Langmuir, by Merrill and Webb, and by Cannara and Crawford, and so the attenuation of the energy of the primaries will take correspondingly longer. Apparently this process is not superefficient, because fast electrons are observed at the anode. Probably the reason is that it is much more difficult for a glow electron to become trapped in a higher energy electron beam because of the velocity mismatch. There are many other questions to be answered, such as why there isn't a uniform reduction of the energy of the primaries instead of some primaries apparently passing through

the glow unchecked (or have they been retarded and then accelerated again?), and we still don't know the detail of the distribution of electron energies in the glow. Although there seems to be sufficient evidence that the glow is the main source of ionization, the reassuring numbers that we calculated for ion-electron pair generation by Maxwellian electrons in the glow would be worthless, and agreement with required rates fortuitous and illusory, if the distribution isn't Maxwellian. Other apparent agreement is also questioned. As we discussed earlier in the chapter, Brewer and Westhaver (1937) obtained excellent agreement between their measured values of negative glow lengths and the ranges of fast electrons obtained by Lehmann (1927), implying a close connection between the two. More recently, Woolsey et al. (1967) have used a magnetic lens arrangement to measure the energies of primary electrons in a helium glow and conclude that the range appears to be less than the length of the glow, contrary to Brewer and Westhaver's conclusion, being as little as two-thirds of the glow length in some cases. I have not been able to obtain a copy of Lehmann's paper yet, but I understand his results for range were obtained in an ionization chamber. In his case there would have been no plasma interaction, and the ranges obtained should therefore be longer than in a plasma using the same initial electron energy.

As a final dampening note, we should consider the probe measurements of Hirsch (1965). Pursuing some earlier observations by Gabor et al. (1955) of electron interactions with oscillations in electrode sheaths, Hirsch concludes that the apparent Maxwellian distribution of electrons, as measured by probes, is more a function of rf interactions in the probe sheath than of the electron energy distribution in the plasma, i.e. that Langmuir's Paradox is not based on reality!

The preceding discussion was intended to give some idea of the difficulties involved in plasma and discharge physics. We should heed the warning given by Cobine (1958) in his introduction, that no sources are infallible, that all proofs should be questioned, and that no discharge phenomena are so well understood that data can be applied precisely. The situation is not significantly different in 1979, at least not in sputtering and plasma etching discharges.

REFERENCES

F. W. Aston, Proc. Roy. Soc. A84, 526 (1911)

D. J. Ball, J. Appl. Phys. 43, 7, 3047 (1972)

D. Barbiere, Phys. Rev. 84, 653 (1951)

D. Bohm and E. P. Gross, Phys. Rev. 75, 1851 (1949); Phys. Rev. 75, 1864 (1949); Phys. Rev. 79, 992 (1950)

A. Keith Brewer and J. W. Westhaver, J. Appl. Phys. 8, 779 (1937)

S. C. Brown, in *Gaseous Electronics*, ed. J. W. McGowan and P. K. John, North-Holland, Amsterdam (1974)

H. Bruining, *Secondary Electron Emission*, Pergamon Press, London (1954)

A. B. Cannara and F. W. Crawford, J. Appl. Phys. 36, 3132 (1965)

C. E. Carlston, G. D. Magnuson, P. Mahadevan, and D. E. Harrison Jr., Phys. Rev. 139A, 729 (1965)

B. N. Chapman, unpublished results (1975)

F. F. Chen, *Introduction to Plasma Physics*, Plenum, New York and London (1974)

J. D. Cobine, *Gaseous Conductors*, Dover, New York (1958)

P. L. Copeland, Thesis, U. of Iowa (1931)

W. D. Davis and T. A. Vanderslice, Phys. Rev. **131**, 219 (1963)

A. J. Dekker, *Solid State Physics*, Macmillan, London (1963)

H. Dreicer, Phys. Rev. **117**, 343 (1960)

M. J. Druvestyn and F. M. Penning, Rev. Mod. Phys. **12**, 88 (1940)

E. W. Eckstein, J. W. Coburn, and Eric Kay, Int. Jnl. of Mass Spec. and Ion Phys. **17**, 129 (1975)

A. von Engel, *Ionized Gases*, Oxford Univ. Press (1965)

A. von Engel and M. Steenbeck, *Elektrische Gasentladungen*, Vols. 1 and 2, Springer, Berlin (1932-4)

K. Fataliev, G. Spivak, and E. Reikhrudel, Zh. eksp. teor. Fiz. **9**, 167 (1939)

G. Francis, in *Handbuch der Physik* **XXII**, ed. S. Flügge, Springer-Verlag, Berlin (1956)

D. Gabor, E. A. Ash, and E. D. Dracott, Nature London **176**, 196 (1955)

F. Howard Gillery, J. Vac. Sci. Tech. **15**, 2, 306 (1978)

A. Güntherschulze, Z. Physik **59**, 433 (1930)

O. Hachenberg and W. Brauer, Adv. in Electronics **11**, 413 (1959)

H. D. Hagstrum, Phys. Rev. **104**, 317 (1956a)

H. D. Hagstrum, Phys. Rev. **104**, 672 (1956b)

H. D. Hagstrum, Phys. Rev. **104**, 1516 (1956c)

H. D. Hagstrum, Phys. Rev. **119**, 940 (1960)

M. Healea and C. Houtermans, Phys. Rev. **58**, 608 (1940)

C. L. Hemenway, R. W. Henry, and M. Caulton, *Physical Electronics*, Wiley and Sons, New York and London (1967)

M. J. Higatsberger, H. L. Demorest, and A. O. Nier, J. Appl. Phys. **25**, 883 (1954)

A. G. Hill, W. W. Buechner, J. S. Clark, and J. B. Fisk, Phys. Rev. **55**, 463 (1939)

E. H. Hirsch, Inter. J. Electronics **19**, 537 (1965)

A. J. T. Holmes and J. R. Cozens, J. Phys. D Appl. Phys. **7**, 1723 (1974)

T. Holstein, Phys. Rev. **70**, 367 (1946)

J. E. Houston and J. E. Uhl, Sandia Research Report, SC-RR-71-0122 (1971)

J. H. Ingold, in *Gaseous Electronics*, Vol. 1, ed. M. N. Hirsh and H. J. Oskam, Academic Press, New York and London (1978)

J. B. Johnson and K. G. McKay, Phys. Rev. **91**, 582 (1953)

J. B. Johnson and K. G. McKay, Phys. Rev. **93**, 668 (1954)

C. Kenty, Phys. Rev. **44**, 891 (1933)

M. Knoll, F. Ollendorff, and R. Rompe, *Gasentladungstabellen*, Verlag Julius Springer, Berlin (1935)

I. Langmuir, Phys. Rev. **26**, 585 (1925)

J. F. Lehmann, Proc. Roy. Soc. **115**, 624 (1927)

R. G. Lye, Phys. Rev. **99**, 1647 (1955)

E. W. McDaniel, *Collision Phenomena in Ionized Gases*, Wiley, New York and London (1964)

K. G. McKay, Adv. in Electronics **1**, 65 (1948)

D. B. Medved, P. Mahadevan, and J. K. Layton, Phys. Rev. **129**, 2086 (1963)

H. J. Merrill and H. W. Webb, Phys. Rev. **55**, 1191 (1939)

E. Nasser, *Fundamentals of Gaseous Ionization and Plasma Electronics*, Wiley Interscience, New York and London (1971)

J. H. Parker, Phys. Rev. **93**, 1148 (1954)

V. Polin and S. D. Gvozdover, Phys. Z. Sowj Un. **13**, 47 (1938)

D. H. Pringle and W. E. J. Farvis, Phys. Rev. **96**, 536 (1954)

D. Rapp and P. Englander-Golden, J. Chem. Phys. **43**, 5, 1464 (1965)

V. K. Rohatgi, J. Appl. Phys. **28**, 951 (1957)

A. Rostagni, Ric. Scient. II/9, **1** (1938)

E. Rudberg, Proc. Roy. Soc. (London) **A127**, 111 (1930)

E. Rudberg, Phys. Rev. **4**, 764 (1934)

E. N. Sickafus, Phys. Rev. B **16**, 1436 (1977); Phys. Rev. B **16**, 1448 (1977)

R. F. Stebbins, Proc. Roy. Soc. **A241**, 270 (1957)

Y. Takeishi and H. D. Hagstrum, Phys. Rev. **137A**, 641 (1965)

J. Thornton, Pub. No. 5885, Litton Industries, Beverly Hills (1967)

T. C. Tisone and P. D. Cruzan, J. Vac. Sci. Tech. **12**, 1058 (1975)

L. Tonks and I. Langmuir, Phys. Rev. **33**, 195 (1929)

N. Wainfan, W. C. Walker, and G. L. Weissler, J. Appl. Phys. 24, 1318 (1953)

G. Wehner, J. Appl. Phys. 21, 62 (1950)

J. Woods, Proc. Phys. Soc. London B67, 843 (1956)

G. A. Woolsey, R. M. Reynolds, and L. P. Clarke, Phys. Letters 25A, 656 (1967)